HHS Public Access

Author manuscript

Eur J Neurosci. Author manuscript; available in PMC 2016 February 25.

Published in final edited form as:

Eur J Neurosci. 2015 May ; 41(11): 1402–1415. doi:10.1111/ejn.12898.

Short-term plasticity regulates the E/I ratio and the temporal window for spike integration in CA1 pyramidal cells

Aundrea F. Bartley and **Lynn E. Dobrunz**

University of Alabama at Birmingham, Department of Neurobiology, Civitan International Research Center, Evelyn F. McKnight Brain Institute, 1825 University Blvd., Birmingham, AL 35294, USA

Abstract

Many neurodevelopmental and neuropsychiatric disorders have an imbalance between excitation (E) and inhibition (I) caused by synaptic alterations. The proper E/I balance is especially critical in CA1 pyramidal cells because they control hippocampal output. Activation of Schaffer collateral axons causes direct excitation of CA1 pyramidal cells, quickly followed by disynaptic feed-forward inhibition, stemming from synaptically induced firing of GABAergic interneurons. Both excitatory and inhibitory synapses are modulated by short-term plasticity, potentially causing dynamic tuning of the E/I ratio. However, the effects of short-term plasticity on the E/I ratio in CA1 pyramidal cells are not yet known. To determine this we recorded disynaptic IPSCs and E/I ratio in CA1 pyramidal cells in acute hippocampal slices from juvenile mice. We find that while inhibitory synapses have paired-pulse depression, disynaptic inhibition instead expresses paired-pulse facilitation (≤ 200 ms intervals), caused by increased recruitment of feed-forward interneurons. Although enhanced disynaptic inhibition helps constrain paired-pulse facilitation of excitation, the E/I ratio is still larger on the second pulse, increasing pyramidal cell spiking. Surprisingly, this occurs without compromising the precision of spike timing. The E/I balance regulates the temporal spike integration window from multiple inputs; here we show that paired-pulse stimulation can broaden the spike integration window. Together, we find that the combined effects of short-term plasticity of disynaptic inhibition and monosynaptic excitation alter the E/I balance onto CA1 pyramidal cells, leading to dynamic modulation of spike probability and spike integration window. Short-term plasticity is therefore an important mechanism for modulating signal processing of hippocampal output.

Keywords

paired-pulse facilitation; disynaptic inhibition; feed-forward inhibition; micee; hippocampus

Introduction

Proper circuit function relies on the correct balance between excitatory and inhibitory synaptic transmission; alterations in this balance can cause circuit dysfunction and disease

Corresponding author: Lynn E. Dobrunz, Ph.D., University of Alabama at Birmingham, 1825 University Blvd., SHEL 902, Birmingham, AL 35294, dobrunz@uab.edu, 205-934-7923.

(Fernandez *et al.*, 2007; Kehrer *et al.*, 2008; Gogolla *et al.*, 2009). However, the ratio of excitatory and inhibitory synaptic transmission (E/I ratio) is not static, but can be modulated by synaptic plasticity. Short-term plasticity causes the strength of both excitatory and inhibitory synapses to be regulated by the temporal pattern of activation (Davies *et al.*, 1990; Zucker & Regehr, 2002). Short-term plasticity also modulates the strength of inputs onto inhibitory interneurons (Wierenga & Wadman, 2003; Sun *et al.*, 2005; Bartley *et al.*, 2008), potentially altering inhibition through changes in interneuron recruitment (Bartos & Elgueta, 2012; Kispersky *et al.*, 2012). The regulation of the E/I ratio by short-term plasticity is therefore complex. Short-term plasticity alters the E/I ratio in cortex (Galarreta & Hestrin, 1998), yet maintains the E/I ratio in the CA3 region of hippocampus (Torborg *et al.*, 2010). The effects of short-term plasticity on the E/I ratio in CA1 pyramidal cells, the main output of hippocampus, are not yet known.

The E/I ratio is important for regulating the overall level of activity in postsynaptic neurons (Carvalho & Buonomano, 2009). It controls the timing of action potentials and regulates the integration of multiple inputs (Wehr & Zador, 2003; Pouille *et al.*, 2009; Isaacson & Scanziani, 2011). The narrow time window during which CA1 pyramidal cells can integrate two sub-threshold inputs to produce spiking becomes extremely broad when inhibition is blocked (Pouille & Scanziani, 2001). Long-term plasticity has been shown to broaden the spike integration window by increasing the strength of excitation relative to inhibition (Lamsa *et al.*, 2005). It remains to be determined whether short-term plasticity can also modulate the spike integration window.

Schaffer collateral excitatory synapses onto CA1 pyramidal cells express robust short-term facilitation (Dobrunz *et al.*, 1997; Dittman *et al.*, 2000). Conversely, monosynaptic IPSCs onto CA1 pyramidal cells have paired-pulse depression (Davies *et al.*, 1990; Klyachko & Stevens, 2006). However, EPSCs onto most CA1 interneurons have short-term facilitation in response to Schaffer collateral stimulation (Wierenga & Wadman, 2003; Sun *et al.*, 2005; Sun *et al.*, 2009), potentially leading to enhanced synaptically evoked spiking and recruitment of interneurons. Short-term plasticity of disynaptic inhibition onto CA1 pyramidal cells has not been studied in depth.

Here we studied the effects of short-term plasticity on disynaptic inhibition, the E/I ratio, and spiking of CA1 pyramidal cells. We find that Schaffer collateral evoked disynaptic IPSCs onto CA1 pyramidal cells have paired-pulse facilitation, caused by increased recruitment of feed-forward interneurons. However, the E/I ratio onto CA1 pyramidal cells is also increased by paired-pulse stimulation, causing an increase in spike probability in CA1 pyramidal cells on the second pulse. Importantly, the enhanced E/I ratio broadens the spike integration window at a short paired-pulse interval. Because short-term plasticity is a ubiquitous feature of synapses that continuously modulates synaptic strength, this is an important mechanism that contributes to frequency-dependent signal processing in hippocampus.

Materials and Methods

Ethical Approval and Slice preparation

Approval was obtained for all experimental protocols from the University of Alabama at Birmingham Institutional Animal Care and Use Committee. All experiments were conducted in compliance with the *Guide for the Care and Use of Laboratory Animals* adopted by the U.S. National Institute of Health. Postnatal day 14 to P20 C57B6/J or FVB mice of either gender were anesthetized with isoflurane, decapitated, and brains rapidly removed. 400 μm thick coronal slices of hippocampus were cut on a vibrating microtome (VT1000S; Leica, Bannockburn, IL) using standard methods (Sun *et al.*, 2005; Sun & Dobrunz, 2006; Sun *et al.*, 2009). Slicing and dissection of the hippocampi were done in ice-cold (1–3 °C) dissecting solution containing the following (in mM): 120 NaCl, 3.5 KCl, 0.75 $CaCl_2$, 4.0 $MgCl_2$, 1.25 NaH_2PO_4, 26 $NaHCO_3$, and 10 glucose, bubbled with 95% O_2/5% CO_2, pH 7.35–7.45. Slices were stored at room temperature in a holding chamber containing the dissecting solution and bubbled with 95% O_2-5% CO_2 for ≥ 1 h before recording.

Electrophysiology

During experiments, slices were held in a submersion recording chamber perfused (2.5–3.5 mLs/min) with external recording solution (ERS). ERS has a similar composition as the dissection solution except for the following (in mM): 2.5 $CaCl_2$ and 1.3 $MgCl_2$. The ERS contained 50 μM D-APV to block NMDA receptor-mediated currents and prevent long-term potentiation and long-term depression. Because some of our experiments involved recording from cells held at 0 mV, the external solution contained 1 μM AM 251 to block CB1 endocannabinoid receptors (De-May & Ali, 2013), in order to prevent changes in the strength of inhibition caused by depolarization induced suppression of inhibition (Pitler & Alger, 1994; Kreitzer & Regehr, 2001; Wilson & Nicoll, 2001). The ERS also contained 10 μM CGP 55845 to block $GABA_B$ receptors and prevent activity dependent reduction in glutamate release from presynaptically localized receptors at Schaffer collateral synapses (Speed & Dobrunz, 2008). Where noted, bicuculline (20 μM) or picrotoxin (1.5 μM or 100 μM) was added to the ERS to reduce or block inhibitory postsynaptic currents (IPSCs) mediated by $GABA_A$ receptors, or 10 μM NBQX was added to the ERS to block excitatory synapses and isolate monosynaptic IPSCs. All experiments were performed between 25°C to 26.5°C.

In all experiments, extracellular stimulation was elicited using a bipolar tungsten microelectrode (FHC, Bowdoinham, ME) placed in *s. radiatum*. Stimulation was generated from a DS8000 digital stimulator (WPI, Sarasota, FL) and applied with a BSI-2 biphasic stimulus isolator (BAK Electronics, Mount Airy, MD). Stimulation was applied as pairs of pulses in a pseudo-random sequence every 10 s; 100 μs duration.

Field Potential Recording

Two field potential recording electrodes were placed in *s. pyramidale*; one less than 75 μm from the stimulation electrode site (Near Stimulation Site) and the other at least 250 μm away from stimulation site (Far from Stimulation Site). The stimulation intensity ranged from 5 μA to 100 μA. The population spike amplitude was calculated by measuring the

amplitude of the negative peak and adding it to the average response size obtained from two positive peaks, as previously described (Marder & Buonomano, 2003).

Pyramidal Whole-Cell Recording

CA1 pyramidal cells were blindly patched on a Nikon (New York, NY) Optiphot-2 upright microscope. Neurons were patched in the voltage-clamp configuration and recorded at various holding potentials (0 mV, −40 mV, and −55 mV) using a Multiclamp 700A amplifier (Molecular Devices, Union City, CA). Patch electrodes (4–6 MΩ) were filled with internal solution composed of the following (in mM): 125 Cs-Gluconate, 0.6 EGTA, 10 Cs-BAPTA, 1.0 $MgCl_2$, 3 $MgSO_4$, 25 HEPES, 2 QX-314, 10 Na-ATP, 0.3 GTP, 5 phospocreatine, pH was adjusted to 7.2 with CsOH. The predicted reversal potential for $GABA_A$ receptors is −58.3 mV (Bormann *et al.*, 1987; Zhang *et al.*, 1991). QX-314 was used to improve space clamp and reduce nonlinear effects caused by voltage-gated channels in dendrites (Colling & Wheal, 1994). Because some of the experiments involved recording from cells held at 0 mV, the internal contained a high concentration (10 mM) of BAPTA to prevent endocannabinoid release (Isokawa & Alger, 2005). The access resistance and holding current (< 200 pA) were monitored continuously. Recordings were rejected if either increased > 30% during the experiment. Postsynaptic currents (PSCs) were recorded in response to extracellular stimulation with the stimulating electrode positioned 250 to 400 μm away from the recording electrode. The stimulation intensity ranged from 8 μA to 55 μA. All of the first pulse measurements were based off the long paired-pulse intervals (500 ms and 1000 ms). In order to isolate the second pulse, for accurate calculation of the paired-pulse ratio, a template of the averaged first pulse was generated and subtracted from the short paired-pulse traces (Figure 1A).

Disynaptic IPSCs and monosynaptic IPSCs were recorded at 0 mV. To limit the amount of monosynaptic contamination in the disynaptic inhibitory responses, the stimulation electrode was placed at least 250–300 μm from the pyramidal cell of interest. Monosynaptic inhibition, measured in the presence of NBQX, made up 13.8 ± 2.8% (n=18) of the total inhibitory current measured at 0 mV, on par with the amount shown in Pouille and Scanziani (2001; Figure 2A, inset). Monosynaptic inhibition was subtracted from the total inhibitory current to obtain a pure disynaptic inhibitory response. Compound PSCs, which contain both excitatory and inhibitory responses, were recorded between −45 mV to −40 mV, which is an intermediate potential between the reversal potential of excitation and inhibition and is close to the action potential firing threshold. In a subset of experiments, after recording the compound PSCs, monosynaptic IPSCs were measured in the presence of NBQX at the holding potential used for the compound PSCs (20.1 ± 6.9% of the total inhibitory current, n=4). The monosynaptic IPSC traces from each interval were averaged together to develop a template. The template monosynaptic IPSC trace was scaled to 20% of the peak of inhibitory component of the compound PSC and then subtracted from the compound PSC to generate a compound PSC that was “free” of monosynaptic IPSC contamination (“monosynaptic-free compound PSC”). The average EPSC was measured in the presence of bicuculline at the same holding potential as the compound PSC, and is referred to as the “underlying EPSC trace”. The underlying EPSC trace is subtracted from the monosynaptic-free compound PSC to obtain the “underlying disynaptic IPSC” trace. The peaks and

charges were measured from the monosynaptic-free compound PS", the underlying EPSC, and the underlying disynaptic IPSC traces to obtain the paired-pulse ratio and excitation to inhibition (E/I) ratio. The latency of responses is measured from the stimulus artifact.

Pyramidal and Interneuron Cell-Attached Recording

Cell-attached recordings were made from either CA1 pyramidal cells or *s. radiatum* interneurons in the voltage-clamp mode following the establishment of high-resistance seal. The observance of unclamped action currents, which were easily detected, indicated action potential firing. Patch electrodes (5–7 MΩ) were filled with internal solution composed of the following (in mM): 130 K-gluconate, 0.1 EGTA, 3 NaCl, 6 KCl, 10 HEPES, 10 Na-ATP, and 0.3 GTP, pH was adjusted to 7.3 with KOH. Interneurons were identified visually in the CA1 *s. radiatum* using infrared differential inference contrast optics on a Nikon (New York, NY) E600FN upright microscope. For cell-attached interneuron recordings, the stimulating electrode was position 75 to 125 um away from the identified interneuron. The stimulus strength was adjusted to generate an action potential firing probability between 0.25 and 0.45.

Cell-attached pyramidal cell recording were used to measure the effects of short-term plasticity on spike probability and spike timing. Cell-attached pyramidal cell recording were also used to measure the spike integration window, as previously described (Pouille & Scanziani, 2001). The spiking integration experiments were performed by stimulating two independent Schaffer collateral pathways subthreshold to action potential firing at various delays (in ms: ± 0, 2, 5, 10, 20, 30, and 50). Paired-pulse stimulation (in ms: 100 or 1000) was applied in conjunction with the various delay intervals. Stimulation on both sides of the cell was to activate different sets of Schaffer collaterals. Independence of the pathways was tested by stimulating a single pulse for each pathway and then testing the two pathways 50 ms apart. If the pathways are independent, then an increase in the spike probability should not be seen when they are stimulated 50 ms apart; if the two electrodes were in the same pathway this would cause an increase in the spike probability of the second pathway due to short-term plasticity. When stimulated alone the pathways had a spike probability of 0.06 ± 0.02 and 0.06 ± 0.03, respectively. When the two pathways were 50 ms apart the spike probability of pathway 1 was 0.07 ± 0.02 and pathway 2 was 0.09 ± 0.02. There was no significant enhancement of the spike probability for either pathway (Paired t-test, Pathway 1 P=0.57, Pathway 2 P=0.22), indicating that they were independent. The spike probability was calculated after the recording for both *s. radiatum* interneurons and CA1 pyramidal cells. In CA1 pyramidal cells, only the spikes from the integrated pulse (second pulse in the sequence) were used for analysis. Latencies were defined as the time between the stimulus artifact and onset of the action potential. The jitter was calculated as the standard deviation of the latency within each cell (Torborg *et al.*, 2010).

Simulation of compound PSCs and E/I ratio

The simulated compound PSC trace was generated from the linear summation of underlying EPSC and IPSC traces obtained during compound PSC recordings, as described above. In order to generate compound PSCs that have paired-pulse depression of disynaptic inhibition, the second pulse in the underlying IPSC trace was scaled to fit the paired-pulse ratio of

monosynaptic inhibition (measured at −45 mV). In a subset of simulations, the latency of the second pulse from the underlying IPSC was altered to match the value seen on the first pulse, thereby removing the delay.

Statistical analysis

All statistics were performed using Origin software (Origin Lab Corporation, 2002) and statistical significance was $p < 0.05$. All asterisks indicate a p-value less than 0.05. Data are presented as mean ± standard error of the mean and sample number (n) refers to cell number. Statistical comparisons for electrophysiological data were made using the Student's *t*-test or paired *t*-test as appropriate or one-way ANOVA followed by Fisher posthoc analysis for multiple comparisons. For the spike integration experiment, a Gaussian fit of the data was performed and the width was used for statistical analysis (Pouille & Scanziani, 2001). The exact P-values are provided in the text for non-significant comparisons.

Results

Schaffer collateral evoked feed-forward inhibition onto CA1 pyramidal cells shows facilitation

Here we determined the overall effect of short-term plasticity on disynaptic feed-forward inhibition in response to Schaffer collateral stimulation. We found that short-term plasticity of disynaptic inhibition onto CA1 pyramidal cells is different from that of monosynaptic inhibition across a range of paired-pulse intervals (Figure 1A–B). Disynaptic and monosynaptic IPSCs were generated in response to stimulation in s. radiatum, with and without 10 μM NBQX, respectively (Figure 1A). The peak response of monosynaptic IPSCs has paired-pulse depression across a range of inter-pulse intervals (Figure 1B). In contrast, the disynaptic IPSCs have robust paired-pulse facilitation of the peaks at intervals up to 200 ms (ANOVA, $F_{9,169}=4.17$, $P<0.002$). Interestingly, disynaptic IPSCs express slight paired-pulse depression at the 1000 ms interval (Student's *t*-test, $P<0.05$), as do monosynaptic IPSCs. Similar effects were seen on the charge transfers of monosynaptic and disynaptic IPSCs (data not shown) (ANOVA, $F_{9,169}=5.59$, $P<0.001$, n=16, 18). Schaffer collateral evoked IPSCs were sensitive to blockade of AMPARs using NBQX (87.2 ± 2.8% blocked, n=18), and had a longer latency than monosynaptic IPSCs by approximately 3 ms (8.1 ± 0.9 ms vs. 5.4 ± 0.4 ms, Student's *t*-test, $P<0.05$), confirming that they are primarily disynaptic. There were no differences in the overall kinetics between monosynaptic and disynaptic IPSCs (Student's *t*-test, $P=0.50$; Table 1). Moreover, there was no difference in the kinetics of the IPSCs between the first and second pulses for either disynaptic IPSCs (ANOVA, $F_{4,650}=0.88$, $P=0.48$; Table 2) or monosynaptic IPSCs (data not shown) (ANOVA, $F_{4,70}=1.00$, $P=0.42$, n=16). However, there was a small increase in latency of the disynaptic IPSC on the second pulse (Paired *t*-test, $P<0.05$; Table 2).

One possible explanation for the difference in short-term plasticity is that Schaffer-collateral evoked disynaptic IPSCs were generated by a different population of interneurons than those recorded for monosynaptic IPSCs. Extracellular stimulation of Schaffer collateral axons is known to activate a wide variety of interneuron types whose dendrites extend into *s. radiatum* (Kajiwara *et al.*, 2008; Katona *et al.*, 2011). Although monosynaptic IPSCs have

generally been shown to have paired-pulse depression (Davies *et al.*, 1990; Klyachko & Stevens, 2006) , previous studies have raised the possibility of subtype-specific differences in short-term plasticity of inhibitory synapses from CA1 interneurons onto pyramidal cells (Jiang *et al.*, 2000; Maccaferri *et al.*, 2000; Bertrand & Lacaille, 2001). Although unlikely, it is possible that the interneurons recruited by Schaffer collateral stimulation to generate disynaptic IPSCs could always express paired-pulse facilitation at their inhibitory synapses onto CA1 pyramidal cells. Therefore, we measured monosynaptic IPSCs from proximal Schaffer collateral stimulation (stimulation near the pyramidal layer) and distal Schaffer collateral stimulation (stimulation near *s. lacunosum-moleculare*) to see if facilitating responses could be observed. Placement of the stimulus near the pyramidal layer mainly activates somatic inhibitory synapses, whereas stimulation near *s. lacunosum-moleculare* targets dendritic inhibitory synapses. We found that both somatic and dendritic targeting inhibitory synapses expressed paired-pulse depression and not paired-pulse facilitation (ANOVA, $F_{9,80}$=1.12, P=0.36; Figure 1C–D). The overall kinetics of the monosynaptic IPSCs from proximal and distal dendritic stimulation were not significantly different (data not shown; Student's *t*-test, P = 0.39; n=10, 8) (Karnup & Stelzer, 1999). Our data suggests that the paired-pulse facilitation of disynaptic inhibition in response to stimulation in the center of *s. radiatum* is unlikely to be due to incorporation of inhibitory synapses located more proximally or more distally that only express paired-pulse facilitation.

Short-term plasticity allows for increased recruitment of stratum radiatum feed-forward interneurons on the second pulse

Short-term facilitation of disynaptic feed-forward inhibition could be caused either by short-term facilitation of the inhibitory synapses or by frequency dependent increases in the probability of interneuron spiking in response to Schaffer collateral stimulation. Since monosynaptic IPSCs onto CA1 pyramidal cells have paired-pulse depression, the paired-pulse facilitation of disynaptic IPSCs onto CA1 pyramidal cells must be caused by an increase in the firing probability of interneurons, and possibly recruitment of additional interneurons that fire at specific frequencies. To test this possibility, we performed cell-attached recordings onto *s. radiatum* interneurons and measured the spike probability during paired-pulse stimulation (Figure 1E–F). The stimulation intensity was set to generate a spike probability between 25 to 45% on the first pulse (29.9% ± 5.2%, n=11, Figure 1F). The average spike latency of the first pulse was 6.5 ± 1.0 ms, consistent with the delay seen in the latency of disynaptic IPSCs as compared to monosynaptic IPSCs (Table 1), although it was highly variable in different cells, ranging from 2 ms to 10.7 ms. The spike timing was precise (jitter 2.1 ± 0.6 ms). An increase in the probability of generating a synaptically driven action potential was seen on the second pulse at all intervals tested (ANOVA, $F_{4,50}$=4.84, P<0.003; Figure 1F) . The effect was robust at short intervals (spike probability was enhanced 2-fold at 20–100 ms). However, there was no significant difference in spike latency on the second pulse (6.7 ± 0.9 ms, Student's *t*-test, P= 0.9) or jitter (2.2 ± 0.9 ms, Student's *t*-test, P = 0.9). Our data suggest that facilitation of disynaptic inhibition onto CA1 pyramidal cells is due to enhanced firing probability of *s. radiatum* interneurons. This is likely to be driven by short-term facilitation of their excitatory inputs (Wierenga & Wadman, 2003; Sun *et al.*, 2005; Sun & Dobrunz, 2006).

In addition to feed-forward inhibition evoked by Schaffer collateral activation, CA1 pyramidal cells also receive feedback inhibition from interneurons excited by local axon collaterals from CA1 pyramidal cells (Takacs *et al.*, 2012). Because many feed-forward interneurons can also participate in feedback inhibition (Freund & Buzsaki, 1996; Klausberger & Somogyi, 2008; Bezaire & Soltesz, 2013), feedback inputs from neighboring CA1 pyramidal cells could potentially contribute to activation of interneurons and thus enhance the IPSCs evoked by Schaffer collateral stimulation. We determined the level of action potential firing from pyramidal cells during paired-pulse stimulation under our recording conditions, using field potential recordings in the *s. pyramidale* at two different locations (Figure S1A). We determined that spiking of CA1 pyramidal cells occurs near the stimulating electrode (within 75 μm) if the stimulation is extremely strong, or at moderate stimulation with short paired-pulse intervals (Figure S1B$_1$). However, little or no spiking was observed for the recording site far from the stimulating electrode (300 to 400 μm away) (Figure S1B$_2$). This suggests that only CA1 pyramidal cells located near the stimulation electrode are likely to fire, and therefore potentially contribute to recruitment of feedback interneurons, during stimulation conditions used to measure disynaptic IPSCs.

Feedback interneurons activated by CA1 pyramidal cells located near the stimulation site potentially have inhibitory synapses targeting the CA1 pyramidal cells being recorded due to axons that project long distances (Freund & Buzsaki, 1996). To determine if feedback inhibition augments paired-pulse facilitation of disynaptic IPSCs, we prevented the ability of Schaffer collateral stimulation to activate nearby CA1 pyramidal cells by placing a small horizontal cut in the slice (McQuiston, 2008) directly below the *s. pyramidale* (Figure S1C). We found that the short-term plasticity of the disynaptic inhibition with reduced feedback inhibition was not significantly different from slices that had intact feedback inhibition, either for the peak (data not shown; ANOVA, $F_{9,145}$=3.74, P=0.06), the charge (Figure S1D, ANOVA, $F_{9,145}$=1.44, P=0.23), or the kinetics (data not shown, Student's t-test, P = 0.43; n=18, 13). Together, these data suggest that feedback inhibition plays at most a minor role in paired-pulse facilitation of disynaptic IPSCs in response to Schaffer collateral stimulation. Similarly, short-term plasticity of mossy fiber evoked IPSCs in CA3 has been shown to be largely independent of feedback inhibition (Torborg *et al.*, 2010). It is possible that activation of feedback inhibition onto CA1 pyramidal cells plays a larger role in response to longer trains or bursts (Elfant *et al.*, 2008).

Short-term plasticity alters the ratio of excitation to disynaptic inhibition in CA1 pyramidal cells in response to Schaffer collateral stimulation

Schaffer collateral excitatory synapses onto CA1 pyramidal cells have robust paired-pulse facilitation (Dobrunz *et al.*, 1997; Dittman *et al.*, 2000; Sun *et al.*, 2005; Christie & Jahr, 2006). Here we have shown that disynaptic IPSCs also have strong paired-pulse facilitation in response to Schaffer collateral stimulation. We next tested what the overall effect of short-term plasticity is on the E/I ratio by measuring compound postsynaptic currents (compound PSCs) from CA1 pyramidal cells. While short-term plasticity of EPSCs and IPSCs have been studied separately (Klyachko & Stevens, 2006; Torborg *et al.*, 2010; Farisello *et al.*, 2012), these experiments directly measure the E/I ratio and interactions between excitation and inhibition. We measured compound PSCs at a holding potential near

the threshold for action potential generation (between −45 mV and −40 mV), which generates a trace with both an EPSC and subsequent IPSC (Figure 2A inset). The excitatory and inhibitory components of the compound PSC were blocked by NBQX (97.7 ± 1.3%, 79.9 ± 6.9%, respectively), indicating that the inhibitory component was primarily a disynaptic response (Pouille & Scanziani, 2001). Both the excitatory and inhibitory components of the compound PSC showed short-term plasticity (Figure 2A). However, the paired-pulse ratio for the excitatory component was much greater than the paired-pulse ratio of the inhibitory component, causing the E/I ratio to be enhanced across a wide range of paired-pulse intervals when assessed by the peaks (ANOVA, $F_{6,91}$=3.27, P<0.006; Figure 2B) or the charge transfer (ANOVA, $F_{6,91}$=2.77, P<0.05; Figure S2A) of the compound PSC. Surprisingly, the E/I ratio was still greatly enhanced at intervals as long as 1000 ms. Although paired-pulse facilitation of the excitatory component is relatively small at the 1000 ms interval (Student's *t*-test, P<0.0002), the inhibitory component expresses a small amount of paired-pulse depression (Student's *t*-test, P<0.03), allowing the E/I ratio to remain enhanced. The enhancement of the E/I ratio on the second pulse was confirmed in separate experiments that measured the peaks of the maximal excitatory and inhibitory responses (at the reversal potentials for GABA and glutamate, respectively), and used these to compute the E/I ratio (ANOVA, $F_{3,24}$=9.09, P<0.0004; Figure S2B) (Torborg *et al.*, 2010). We also tested the effects of short term plasticity on the E/I ratio in the absence of blockers of NMDA receptors, CB1 receptors, and $GABA_B$ receptors, and found that the responses were not different from the responses measured in the presence of these antagonists for the first pulse or second pulses (ANOVA, $F_{7,32}$=0.55, P=0.79; Figure S2C). In addition, there was no difference in the E/I ratio (at any of the intervals) caused by blocking only NMDA receptors (ANOVA, $F_{7,24}$=0.23, P=0.97; Figure S2D), consistent with a previous study (Zhang *et al.*, 2011). While this does not rule out a possible role for NMDA receptors, CB1 receptors, or $GABA_B$ receptors in regulating the E/I ratio in CA1 pyramidal cells under some conditions (e.g. longer trains, (Dubruc *et al.*, 2013; Zachariou *et al.*, 2013), it indicates that paired-pulse facilitation of the E/I ratio is not dependent upon blocking these receptors, and occurs under more physiological conditions. Together, these data show that although disynaptic IPSCs are enhanced in response to short-term plasticity, the E/I ratio onto CA1 pyramidal cells during the second pulse is still larger than the E/I ratio obtained on the first pulse. This is the first direct demonstration that short-term plasticity alters the ratio of excitation to inhibition of the compound PSC in CA1.

We measured the underlying EPSCs of the compound PSCs by blocking $GABA_A$ receptors with bicuculline (Figure 2C). We also calculated the underlying IPSCs by subtracting the EPSC (measured in bicuculline) from the compound PSC (Pouille & Scanziani, 2001; Gabernet *et al.*, 2005). The paired-pulse ratio of the excitatory component of the compound PSC (Figure 2A) was greater than that of the underlying EPSC (ANOVA, $F_{11,60}$=3.79, $P<0.0004$; Figure 2D), indicating that interactions between inhibition and excitation enhances short-term facilitation of Schaffer collateral excitatory inputs to CA1 pyramidal cells, consistent with a previous study (Klyachko & Stevens, 2006). However, our results suggest that this is not caused by paired-pulse depression of inhibition, because disynaptic IPSCs have paired-pulse facilitation (Figures 1B, 2D). In contrast to excitation, the magnitude of paired-pulse facilitation of the inhibitory component (Figure 2A) is similar to

that of the underlying disynaptic inhibition (ANOVA, $F_{11,60}$=1.98, P=0.12; Figure 2D), indicating that interactions with excitation do not alter the short-term plasticity of inhibition. Additionally, the latency of the underlying IPSC was greater on the second pulse compared to the first pulse at short intervals (ANOVA, $F_{6,35}$=3.56, P<0.008; Figure 2E).

The underlying EPSC indicates the maximum amount of excitation generated onto the pyramidal cell in response to that particular Schaffer collateral stimulation. Because the excitatory peak of the compound PSC is less than the maximum EPSC, we calculated the percentage of the underlying EPSC that is transmitted during the compound PSC by dividing the amplitude of the compound excitatory component by the peak of the underlying EPSC. On the first pulse approximately 75% of the underlying EPSC was transmitted in the compound PSC (dash-dotted line in Figure S2E). This was increased to nearly 95% on the second pulse at short intervals (Figure S2E). This interaction between excitation and inhibition enhances the paired-pulse ratio of the excitatory component of the compound PSC compared to the underlying EPSC.

The excitatory components of compound PSCs are the synaptic inputs necessary to generate action potential firing, and the summation of several excitatory synaptic responses is necessary to reach the spike threshold for CA1 pyramidal cells (Otmakhov *et al.*, 1993). The length of time that the compound PSC is depolarizing (excitatory) is dependent upon the onset and strength of the hyperpolarizing (inhibitory) component (Gabernet *et al.*, 2005; Chittajallu *et al.*, 2012). We find that the excitation window (the time window during which the compound PSC is depolarizing (excitatory), as shown in Figure 2C by line ‘a’) is broader for the second pulse of the compound PSCs across a wide range of paired-pulse intervals (ANOVA, $F_{6,91}$=3.30, P<0.006; Figure 2F). These data show that short-term plasticity modulates several aspects of the compound PSC, including the E/I ratio and the excitation window.

Simulated compound PSCs estimate the extent to which paired-pulse facilitation of inhibition restrains the enhancement of the E/I ratio and excitation window

We estimated how short-term plasticity would alter the E/I ratio if disynaptic inhibition expressed paired-pulse depression and not facilitation, using summation of recorded EPSC traces and modified IPSC traces. Figure 3A shows the control compound PSC averaged from 6 experiments at the 100 ms interval; the disynaptic IPSC had both paired-pulse facilitation of inhibition and a longer latency on the second pulse (Control (PPF)). Figure 3A also shows the average of simulated traces generated from the average underlying EPSC and IPSC traces from the same experiments, but with the amplitude of the IPSC on the second pulse scaled to give a paired-pulse ratio of 0.77 (PPD of inhibition). Scaling the underlying IPSC to have paired-pulse depression causes a reduction of the inhibitory peak of the simulated compound PSCs on the second pulse. This results in a 7-fold increase in the E/I ratio on the second pulse at 100 ms, which is much larger than the 2-fold increase observed experimentally (Student’s *t*-test, P<0.05; Figure 3B, Control (PPF)). Paired-pulse depression of inhibition also greatly enhances the duration that the compound PSC is excitatory (excitation window, Student’s *t*-test, P<0.05; Figure 3C), and increases the amount of paired-pulse facilitation of the excitatory component of the compound PSC (Student’s *t*-test,

$P<0.05$; Figure 3D). The fact that disynaptic inhibition has paired-pulse facilitation, rather than paired-pulse depression as occurs with monosynaptic inhibition, is important for constraining the increase in E/I ratio and excitation window on the second pulse.

We next used simulations to test the effect of the longer latency of disynaptic inhibition (delay) on the second pulse by generating simulated compound PSCs using underlying IPSCs that had the same observed amount of paired-pulse facilitation but were shifted to remove the delay on the second pulse (PPF of inhibition no delay, Figure 3E). Removing the delay on the second pulse of disynaptic inhibition decreased the paired-pulse facilitation of the excitatory component of the compound PSCs (Student's *t*-test, $P<0.05$; Figure 3H) without altering the E/I ratio or excitation window (Student's *t*-test, $P>0.18$; Figure 3F,G). The latency in the onset of inhibition regulates the amount of excitation that is transmitted in the compound PSC; the increase in latency (delay) of inhibition on the second pulse causes the paired-pulse ratio of the excitatory component to be larger than that of the underlying EPSC. These results suggest that the differences observed between disynaptic and monosynaptic inhibition (paired-pulse facilitation, longer latency on second pulse) are important to constrain the increases in E/I ratio and the excitation window, while increasing the paired-pulse ratio of the excitatory component.

Short-term plasticity enhances spiking and alters spike jitter

We next tested the effects of short-term plasticity on pyramidal cell spiking in response to paired-pulse stimulation of Schaffer collateral axons. Since short-term plasticity of excitation and disynaptic inhibition onto CA1 pyramidal cells are not equivalent and the E/I ratio is enhanced at short paired-pulse intervals, we predicted that short-term plasticity would increase the spike output of CA1 pyramidal cells. Experiments using cell attached recordings from CA1 pyramidal cells (Figure 4A) showed that paired-pulse facilitation of the E/I ratio caused the spike probability on the second pulse to more than double at a short (100 ms) paired-pulse interval (ANOVA, $F_{2,30}=48.05$, $P<0.006$; Figure 4B). Furthermore, the spike probability was still increased in response to short term plasticity when the second pulse was 1000 ms later than the first pulse, consistent with the enhanced E/I ratio at this interval (Figure 2B). The enhanced spiking was accompanied by a small decrease in spike latency at the 100 ms interval but not the 1000 ms interval (ANOVA, $F_{2,30}=3.91$, $P<0.04$; Figure 4C). Together, these data indicate that the effect of short-term plasticity to increase the E/I ratio can greatly increase CA1 output across a wide range of intervals, a wider range than has been previously investigated (Leung & Fu, 1994).

Previous studies have shown that enhanced spiking caused by increasing the E/I ratio is accompanied by a decrease in the precision of spike timing, seen as an increase in spike jitter (Pouille & Scanziani, 2001; Lamsa *et al.*, 2005). Surprisingly, the increase in spiking caused by short-term plasticity was instead accompanied by a decrease in spike jitter on the second pulse at 100 ms, with no significant change in spike jitter observed on the second pulse at 1000 ms (ANOVA, $F_{2,30}=4.86$, $P<0.02$; Figure 4D). Because the E/I ratio is enhanced at both intervals, this shows that increasing the E/I ratio does not always cause an increase in spike jitter. The fact that the spike jitter was actually reduced on the second pulse

(despite the increase in the spike probability), suggests that paired-pulse facilitation of disynaptic inhibition helps maintain the precision of spike timing.

To further test this, we blocked inhibition using 100 μM picrotoxin, which increased the spike probability on the first pulse to 0.90 ± 0.06 (n=4) and greatly enhanced the spike jitter compared to stimulating at the same intensity with inhibition intact (Student's *t*-test, $P<0.05$; Figure 4E). The increased spike jitter was not simply a result of the larger spike probability, because a similarly high spike jitter was seen when the stimulus intensity was reduced to return the spike probability back to its initial level (0.42 ± 0.04, n=4) (Figure 4E). These data are consistent with the known importance of inhibition for regulating spike timing (Pouille & Scanziani, 2001). We then tested the effects of blocking inhibition (at the reduced stimulus intensity) on pyramidal cell spiking during paired-pulse stimulation. With inhibition completely blocked, the spike probability was enhanced on the second pulse at both 100 ms and 1000 ms intervals (ANOVA, $F_{2,9}=12.42$, $P<0.003$; Figure 4F) to a similar degree as when inhibition was intact (Figure 4B). There was also a small decrease in spike latency on the second pulse at 100 ms (Paired *t*-test, $P<0.05$; Figure 4G). However, the spike jitter was the same on pulse 1 and pulse 2 (ANOVA, $F_{2,9}=0.09$, $P=0.91$; Figure 4H), indicating that paired-pulse facilitation of EPSCs alone does not modulate spike jitter.

With inhibition intact, the E/I ratio (Figure 2B) and spike probability (Figure 4B) were about twice as large on the second pulse at 100 ms compared to the first pulse. We tested the effect of doubling the size of the E/I ratio by partially blocking inhibition. Dose response experiments determined that 1.5 μM picrotoxin caused approximately a 50% block of inhibition (Figure 4I). Using 1.5 μM picrotoxin to increase the E/I ratio caused a similar increase in the probability of spiking (Paired *t*-test, $P<0.05$; Figure 4J) as had been observed on the second pulse at 100 ms with inhibition intact (Figure 4B). However, increasing the E/I ratio by reducing inhibition caused a large increase in spike jitter (Paired *t*-test, $P<0.05$; Figure 4K), rather than a decrease as was seen with short-term plasticity. Together, these results show that spike jitter is not controlled strictly by the E/I ratio, but also by the strength of inhibition. As a result, paired-pulse facilitation of disynaptic inhibition helps to maintain the precision of spike timing even though short-term plasticity increases the E/I ratio and enhances spike output.

Short-term plasticity alters the spiking integration window

Finally, we tested whether short-term plasticity of feed-forward inhibition could influence the time window over which CA1 pyramidal cells can integrate multiple sub-threshold inputs to produce an action potential. This window has been shown to be critically dependent upon the strength of feed-forward inhibition (Pouille & Scanziani, 2001; Lamsa *et al.*, 2005; Tsukada *et al.*, 2005). We recorded from CA1 pyramidal cells in cell-attached mode and measured the spike integration window using two stimulation electrodes stimulated either simultaneously (0 ms delay) or with delays of ± 2 to 50 ms. Example traces are shown in Figure 5B. Stimulation electrodes were placed in *s. radiatum* approximately 300 to 400 μm on either side of the neuron (Figure 5A) to activate independent sets of Schaffer collateral axons. Stimulation intensity was set so that when the two Schaffer collateral pathways were simultaneously stimulated the pyramidal cell fired an action

potential on the first pulse 30 to 50% of the time (Figure 5C, stimulus intensity 20.6 ± 2.3 μA). Each pathway stimulated separately was sub-threshold for firing action potentials on the first pulse, although not always on the second pulse (data not shown).

We found that the spike probability was greatly enhanced on the second pulse compared to the first pulse at both the 100 ms paired-pulse interval and 1000 ms interval when both stimulations were simultaneous ($_{ANOVA}$, $F_{2,25}$=17.1, p<0.0005; Figure 5C), consistent with the results from Figure 4B. This was accompanied by a decrease in spike latency and jitter on the second pulse at 100 ms (Paired *t*-test, *P*<0.05) but not 1000 ms (Paired *t*-test, *P*=0.48) (Figure 5E). The spike probability was also enhanced by paired-pulse stimulation over a wide range of delays at both paired-pulse intervals (Figure 5D), with the effect being larger at the 100 ms interval (Figure $5D_1$). Finally, we tested for effects of short-term plasticity on the spike integration window by plotting the data from Figure 5D normalized to the maximum spike probability at 0 ms delay (Figure 5F) (Pouille & Scanziani, 2001). At the 100 ms paired-pulse interval the spike integration window was broader on the second pulse compared to the first, based on a Gaussian fit of the data ($_{ANOVA}$, $F_{2,25}$=5.62, p<0.01; Figure 5G). However, at the 1000 ms paired-pulse interval the spike integration window remained the same between the first and second pulse ($_{ANOVA}$, $F_{2,25}$=5.62, p<0.01; Figure 5G). Enhancing the spike probability and altering the spike integration window will fundamentally alter how information is processed as a function of frequency. This is a new role for short-term plasticity in regulating circuit function.

Discussion

Here we show that short-term plasticity regulates the strength of disynaptic inhibition and the E/I ratio in CA1 of hippocampus. While monosynaptic IPSCs have paired-pulse depression, short-term plasticity enhances disynaptic inhibition, resulting in facilitation of feed-forward inhibition on the second pulse at intervals ≤ 200 ms. Paired-pulse facilitation of disynaptic inhibition is primarily due to increased recruitment of feed-forward interneurons and not incorporation of feedback inhibition on the second pulse. The facilitation of disynaptic inhibition is less than that of excitation, resulting in an overall increase in the E/I ratio in CA1 pyramidal cells. The enhanced E/I ratio leads to an increase in action potential firing of pyramidal cells on the second pulse and slightly broadens the integration window while still being able to maintain spike precision.

Short-term plasticity of excitation and inhibition, and the interaction between the two, causes the E/I ratio onto CA1 pyramidal cells to be dynamically enhanced across a wide range of paired-pulse intervals, although the role of disynaptic inhibition in this effect is different at long intervals. At short paired-pulse intervals, paired-pulse facilitation of both excitation and inhibition are robust, but facilitation of excitation is greater, resulting in a larger E/I ratio and enhanced spiking. In this case, paired-pulse facilitation of inhibition helps constrains the increase in E/I ratio that would otherwise result from facilitation of excitation. Simulations suggest that the E/I ratio would be more than three times larger at the 100 ms interval if disynaptic inhibition had paired-pulse depression instead of paired-pulse facilitation. If there was paired-pulse depression of inhibition at short intervals, it would greatly increase the E/I ratio and cause higher frequency firing that could possibly saturate

hippocampal output. Surprisingly, the E/I ratio in CA1 pyramidal cells is still elevated on the second pulse at the 1000 ms interval. Although paired-pulse facilitation of the excitatory component of the compound PSC is only slightly facilitated, the disynaptic inhibitory component now expresses paired-pulse depression. Together, this causes facilitation of the E/I ratio at this interval. Short-term plasticity (paired-pulse depression) of disynaptic inhibition contributes to, rather than opposes, the increase in E/I ratio on the second pulse at the 1000 ms interval.

The increase in the E/I ratio in CA1 by short-term plasticity differs from the CA3 region, where the E/I ratio from mossy-fiber synapses onto CA3 pyramidal cells remains constant during short-term plasticity (Torborg *et al.*, 2010). However, longer trains of high frequency stimulation have been shown to increase the ratio of E/I onto pyramidal cells in CA3 (Thompson & Gahwiler, 1989) and in somatosensory cortex (Gabernet *et al.*, 2005). The E/I ratio can also decrease during high frequency stimulation in cortex (Galarreta & Hestrin, 1998; Varela *et al.*, 1999). The effects of short-term plasticity on the E/I ratio are therefore highly specialized, being both input dependent and region dependent. These specializations enable differential tuning of neurons for specific functions based on the relative effects of short-term plasticity on excitation and inhibition.

It has previously been shown that changes in the E/I ratio caused by long-term plasticity can modulate spike output (Lamsa *et al.*, 2005; Carvalho & Buonomano, 2009). Here we find that modulation of the E/I ratio by short-term plasticity enhances the spike probability in CA1 pyramidal cells on the second pulse at both short and long paired-pulse intervals. Although short-term plasticity increases the spiking of CA1 pyramidal cells in hippocampus (Leung & Fu, 1994), in cortex the frequency-dependent decrease in E/I instead reduces spiking and stabilizes the network during periods of high activity (Galarreta & Hestrin, 1998; Varela *et al.*, 1999). Additionally, matched short-term plasticity of excitation and inhibition in hippocampal CA3 pyramidal cells (Torborg *et al.*, 2010) helps maintain the rhythmic firing necessary for oscillation generation and transferring information (Atallah & Scanziani, 2009; Economo & White, 2012; Zemankovics *et al.*, 2013). By altering the effectiveness of inhibition to regulate CA1 output, short-term plasticity may be an important mechanism that tunes CA1 cells to fire at specific frequencies (Sasaki *et al.*, 2006), or encode order selectivity of neural responses (Goudar & Buonomano, 2014).

Feed-forward inhibition strongly regulates the temporal window needed to summate synaptic activity (Pouille & Scanziani, 2001; Lamsa *et al.*, 2005; Luna & Schoppa, 2008). Here we show for the first time that short-term plasticity can regulate the spike integration window in CA1 pyramidal cells. The spike integration window is wider at the 100 ms interval, but not the 1000 ms interval, indicating that the effect is frequency-dependent. The broadening of the spike integration window allows multiple inputs that are less coincident to trigger action potentials in CA1 pyramidal cells. A slight broadening of the integration window during paired-pulse stimulation therefore helps CA1 pyramidal cells to function more effectively as integrators. However, the spike integration window in response to short-term plasticity is still much narrower than when inhibition is completely abolished (Pouille & Scanziani, 2001). The fact that disynaptic feed-forward inhibition onto CA1 pyramidal cells has paired-pulse facilitation should help to constrain the increase in the E/I ratio on the

second pulse (Figure 3B), which should prevent a much larger broadening of the spike integration window that could potentially compromise circuit function. Instead, the effects of short-term plasticity on the E/I balance may dynamically shift the function of the CA1 pyramidal cell between integration and coincidence detection depending on the input frequency.

Feed-forward inhibition can regulate the precision of spike timing. Blocking inhibition increases the spike jitter, thereby reducing the temporal precision of spiking (Pouille & Scanziani, 2001). Increasing the E/I ratio through long-term plasticity also reduces the fidelity of spike timing (Lamsa *et al.*, 2005). However, short-term plasticity does not compromise the precision of spike timing when the E/I ratio is altered by paired-pulse stimulation, and actually reduces spike jitter on the second pulse at 100 ms (Figure 4D, 5E). This indicates that the broadening of the spike integration window does not always compromise spike fidelity. One difference is that in the previous studies the magnitude of inhibition was reduced (Lamsa *et al.*, 2005) or completely blocked (Pouille & Scanziani, 2001). Consistent with this, we see a large increase in spike jitter when inhibition is completely blocked (Figure 4E, H). Furthermore, when the E/I ratio was increased by low dose picrotoxin to a similar extent (e.g. 2 fold) as was observed with paired-pulse stimulation, this also caused an increase in spike jitter (Figure 4K). This indicates that spike precision is not regulated solely by the E/I ratio, but also by the magnitude of inhibition. Together our results suggest that facilitation of disynaptic feed-forward inhibition is important for maintaining spike precision in CA1 pyramidal cells, which is important for regulating long-term synaptic strength through spike timing dependent plasticity.

Our results indicate that short-term plasticity of disynaptic inhibition is not determined by the dynamics of the inhibitory synapses themselves. Although it is often assumed that all CA1 feed-forward interneurons are reliably recruited to fire by their excitatory inputs, as shown for CA3 interneurons (Miles, 1990), we show here, and others have demonstrated (e.g. Maccaferri & Dingledine, 2002), that stimulation of Schaffer collateral axons does not always cause action potential firing of *s. radiatum* interneurons. As a result, their firing probability can be dynamically modulated by short-term plasticity. The frequency-dependent increases in the recruitment of feed-forward interneurons can counteract the short-term depression of their inhibitory outputs, causing paired-pulse facilitation. We show that disynaptic inhibition is facilitated at intervals up to 200 ms. Consistent with this, spiking of inhibitory interneurons is also facilitated at intervals up to 200 ms. However, at longer paired-pulse intervals, disynaptic inhibition has paired-pulse depression, similar to that of monosynaptic inhibition, consistent with the idea that there is no longer enhanced recruitment of interneurons on the second pulse. We and others have previously shown that most interneurons in *s. radiatum* have paired-pulse facilitation of their Schaffer collateral inputs (Wierenga & Wadman, 2003; Sun *et al.*, 2005; Sun *et al.*, 2009), which most likely underlies the paired-pulse facilitation of their spiking seen at shorter intervals. This does not rule out possible contributions of a change in EPSP-spike coupling on the second pulse and/or reduced inhibition onto the interneurons. The role of short-term plasticity in regulating the E/I ratio onto interneurons remains to be explored.

Different classes of interneurons have been shown to be activated at various frequencies (Klausberger & Somogyi, 2008). We observed an increase in the latency of disynaptic inhibition, but not monosynaptic inhibition, on the second pulse. However, we did not see an increase in the latency of spiking of *s. radiatum* inhibitory interneurons on the second pulse, although the variability was large. This could indicate that a different population of interneurons is being recruited on the second pulse. One limitation of our study is that it was not possible to determine the molecular identity of the interneurons that contributed to Schaffer collateral evoked disynaptic inhibition. *S. radiatum* interneurons are a diverse population of primarily dendritic targeting interneurons (Freund & Buzsaki, 1996; Klausberger, 2009; Bezaire & Soltesz, 2013), most of which express paired-pulse facilitation with Schaffer collateral inputs (Wierenga & Wadman, 2003; Sun *et al.*, 2005; Sun *et al.*, 2009), leading to increased spiking. As a result, the strength of dendritic inhibition is likely to be larger on the second pulse. Schaffer collateral stimulation also evokes firing of parvalbumin and cholecystokinin basket cells in *s. pyramidale* that provide perisomatic inhibition to CA1 pyramidal cells (Wierenga & Wadman, 2003; Glickfeld & Scanziani, 2006; Owen *et al.*, 2013). However, increases in basket cell recruitment are not likely to contribute to the observed paired-pulse facilitation of disynaptic inhibition because parvalbumin basket cells fire reliably, while the firing of cholecystokinin basket cells should decrease on the second pulse (Pouille *et al.*, 2009; Bartos & Elgueta, 2012; Campanac *et al.*, 2013), leading to a decrease in somatic inhibition. A weakening of somatic inhibition and strengthening of dendritic inhibition during periods of high activity has been previously shown for feedback inhibition onto CA1 pyramidal cells (Pouille & Scanziani, 2004) and for feed-forward inhibition onto dentate gyrus interneurons (Liu *et al.*, 2014). A similar activity dependent shift between somatic and dendritic inhibition may occur for feed-forward inhibition onto CA1 pyramidal cells.

Somatic recordings are known to underestimate the size of synaptic currents due to the difficulty of maintaining a constant voltage clamp in the dendrites. Because excitatory synapses are on the dendrites, while inhibitory synapses are on the soma and dendrites, space clamp errors are likely to cause an underestimation of the E/I ratio (Williams & Mitchell, 2008). The effects are likely to be largest on the second pulse during short paired-pulse intervals, where large paired-pulse facilitation of excitation could depolarize the dendrites despite voltage clamp at the soma. As a result, the E/I ratio might actually be more frequency-dependent than was observed. In addition, the enhanced E/I ratio at 1000 ms causes enhanced spiking of CA1 pyramidal cells even when inhibition is completely blocked. This suggests that there is still paired-pulse facilitation of excitation at the 1000 ms interval, although that was not observed in paired-pulse somatic voltage clamp recordings of EPSCs. Therefore, it is likely that we are underestimating the paired-pulse facilitation of excitation due to space clamp errors (Williams & Mitchell, 2008).

Although we looked at simple forms of short-term plasticity, Schaffer collateral synapses in vivo receive longer spike trains that are very temporally complex (Fenton & Muller, 1998). It has previously been shown that multiple forms of short-term plasticity interact to cause large rapid changes in synaptic strength during behaviorally salient input patterns (Dobrunz & Stevens, 1999; Ohliger-Frerking *et al.*, 2003; Dekay *et al.*, 2006) As a result, the E/I ratio

onto CA1 pyramidal cells is likely to continually change depending upon stimulus frequency (Klyachko & Stevens, 2006), which could cause dynamic changes to spike probability and the spike integration window.

In this study we investigated the effects of short-term plasticity on the E/I ratio in CA1 pyramidal cells from slices taken from juvenile mice. However, it is possible that the effects of short-term plasticity on the E/I ratio are developmentally regulated. Developmental changes have been shown to occur in short-term plasticity of many excitatory synapses (Ramoa & Sur, 1996; Feldmeyer & Radnikow, 2009; Chen & Buonomano, 2012), including excitatory inputs to CA1 pyramidal cells (Hussain & Carpenter, 2001; Dekay *et al.*, 2006; Speed & Dobrunz, 2008; 2009). Less is known about possible developmental changes in short-term plasticity of excitatory inputs onto interneurons, or short-term plasticity of inhibitory synapses (Ingram *et al.*, 2008; Grantyn *et al.*, 2011; Venkataraman & Bartlett, 2013). All of these factors could potentially result in developmental changes in short-term plasticity of the E/I balance onto CA1 pyramidal cells, as has been observed for mossy fiber inputs onto CA3 pyramidal cells (Torborg *et al.*, 2010). It remains to be determined if there are developmental changes in short-term plasticity of the E/I balance of Schaffer collateral evoked inputs onto CA1 pyramidal cells.

In summary, we have shown that at short intervals, paired-pulse modulation of the E/I ratio increases the spike probability and broadens the spike integration window on the second pulse. Short-term plasticity causes facilitation of disynaptic feed-forward inhibition onto CA1 pyramidal cells, which helps to constrain the increase in the E/I ratio that occurs from robust paired-pulse facilitation of excitation. The enhancement of feed-forward inhibition also maintains spiking precision of CA1 pyramidal cells. At longer intervals, paired-pulse depression of inhibition helps to enhance the E/I ratio and increase spiking even though paired-pulse facilitation of excitation is small. However, the increase in the E/I ratio does not change the spike integration window at longer intervals. As a result, short-term plasticity can enhance the output of CA1 pyramidal cells while controlling the extent to which they act as integrators or coincidence detectors at various frequencies.

Supplementary Material

Refer to Web version on PubMed Central for supplementary material.

Acknowledgments

This work was supported by National Institutes of Health grants R56MH065328 and R01MH098534 to L.E.D., a Civitan International Research Center Emerging Scholars Award to A.F.B., and the Evelyn F. McKnight Brain Institute. We would like to thank Drs. Qin Li, Lori McMahon, Linda Overstreet-Wadiche, Kristina Visscher, and Jacques Wadiche for their critical reading and helpful comments on this manuscript.

Abbreviations

E	Excitation
EPSCs	Excitatory Postsynaptic Currents

ERS	External Recording Solution
I	Inhibition
IPSCs	Inhibitory Postsynaptic Currents
PPD	Paired-Pulse Depression
PPF	Paired-Pulse Facilitation
PSCs	Postsynaptic Currents

References

Atallah BV, Scanziani M. Instantaneous modulation of gamma oscillation frequency by balancing excitation with inhibition. Neuron. 2009; 62:566–577. [PubMed: 19477157]

Bartley AF, Huang ZJ, Huber KM, Gibson JR. Differential activity-dependent, homeostatic plasticity of two neocortical inhibitory circuits. Journal of neurophysiology. 2008; 100:1983–1994. [PubMed: 18701752]

Bartos M, Elgueta C. Functional characteristics of parvalbumin- and cholecystokinin-expressing basket cells. The Journal of physiology. 2012; 590:669–681. [PubMed: 22250212]

Bertrand S, Lacaille JC. Unitary synaptic currents between lacunosum-moleculare interneurones and pyramidal cells in rat hippocampus. The Journal of physiology. 2001; 532:369–384. [PubMed: 11306657]

Bezaire MJ, Soltesz I. Quantitative assessment of CA1 local circuits: knowledge base for interneuron-pyramidal cell connectivity. Hippocampus. 2013; 23:751–785. [PubMed: 23674373]

Bormann J, Hamill OP, Sakmann B. Mechanism of anion permeation through channels gated by glycine and gamma-aminobutyric acid in mouse cultured spinal neurones. The Journal of physiology. 1987; 385:243–286. [PubMed: 2443667]

Campanac E, Gasselin C, Baude A, Rama S, Ankri N, Debanne D. Enhanced intrinsic excitability in basket cells maintains excitatory-inhibitory balance in hippocampal circuits. Neuron. 2013; 77:712–722. [PubMed: 23439123]

Carvalho TP, Buonomano DV. Differential effects of excitatory and inhibitory plasticity on synaptically driven neuronal input-output functions. Neuron. 2009; 61:774–785. [PubMed: 19285473]

Chen WX, Buonomano DV. Developmental shift of short-term synaptic plasticity in cortical organotypic slices. Neuroscience. 2012; 213:38–46. [PubMed: 22521823]

Chittajallu R, Pelkey KA, McBain CJ. Neurogliaform cells dynamically regulate somatosensory integration via synapse-specific modulation. Nature neuroscience. 2012; 16:13–15. [PubMed: 23222912]

Christie JM, Jahr CE. Multivesicular release at Schaffer collateral-CA1 hippocampal synapses. The Journal of neuroscience : the official journal of the Society for Neuroscience. 2006; 26:210–216. [PubMed: 16399689]

Colling SB, Wheal HV. Fast sodium action potentials are generated in the distal apical dendrites of rat hippocampal CA1 pyramidal cells. Neurosci Lett. 1994; 172:73–96. [PubMed: 8084540]

Davies CH, Davies SN, Collingridge GL. Paired-pulse depression of monosynaptic GABA-mediated inhibitory postsynaptic responses in rat hippocampus. The Journal of physiology. 1990; 424:513–531. [PubMed: 2167975]

De-May CL, Ali AB. Cell type-specific regulation of inhibition via cannabinoid type 1 receptors in rat neocortex. Journal of neurophysiology. 2013; 109:216–224. [PubMed: 23054605]

Dekay JG, Chang TC, Mills N, Speed HE, Dobrunz LE. Responses of excitatory hippocampal synapses to natural stimulus patterns reveal a decrease in short-term facilitation and increase in short-term depression during postnatal development. Hippocampus. 2006; 16:66–79. [PubMed: 16261553]

Dittman JS, Kreitzer AC, Regehr WG. Interplay between facilitation, depression, and residual calcium at three presynaptic terminals. The Journal of neuroscience : the official journal of the Society for Neuroscience. 2000; 20:1374–1385. [PubMed: 10662828]

Dobrunz LE, Huang EP, Stevens CF. Very short-term plasticity in hippocampal synapses. Proceedings of the National Academy of Sciences of the United States of America. 1997; 94:14843–14847. [PubMed: 9405701]

Dobrunz LE, Stevens CF. Response of hippocampal synapses to natural stimulation patterns. Neuron. 1999; 22:157–166. [PubMed: 10027298]

Dubruc F, Dupret D, Caillard O. Self-tuning of inhibition by endocannabinoids shapes spike-time precision in CA1 pyramidal neurons. Journal of neurophysiology. 2013; 110:1930–1944. [PubMed: 23904493]

Economo MN, White JA. Membrane properties and the balance between excitation and inhibition control gamma-frequency oscillations arising from feedback inhibition. PLoS Comput Biol. 2012; 8:e1002354. [PubMed: 22275859]

Elfant D, Pal BZ, Emptage N, Capogna M. Specific inhibitory synapses shift the balance from feedforward to feedback inhibition of hippocampal CA1 pyramidal cells. The European journal of neuroscience. 2008; 27:104–113. [PubMed: 18184315]

Farisello P, Boido D, Nieus T, Medrihan L, Cesca F, Valtorta F, Baldelli P, Benfenati F. Synaptic and extrasynaptic origin of the excitation/inhibition imbalance in the hippocampus of synapsin I/II/III knockout mice. Cerebral cortex. 2012; 23:581–593. [PubMed: 22368083]

Feldmeyer D, Radnikow G. Developmental alterations in the functional properties of excitatory neocortical synapses. J Physiol. 2009; 587:1889–1896. [PubMed: 19273572]

Fenton AA, Muller RU. Place cell discharge is extremely variable during individual passes of the rat through the firing field. Proc Natl Acad Sci U S A. 1998; 95:3182–3187. [PubMed: 9501237]

Fernandez F, Morishita W, Zuniga E, Nguyen J, Blank M, Malenka RC, Garner CC. Pharmacotherapy for cognitive impairment in a mouse model of Down syndrome. Nature neuroscience. 2007; 10:411–413. [PubMed: 17322876]

Freund TF, Buzsaki G. Interneurons of the hippocampus. Hippocampus. 1996; 6:347–470. [PubMed: 8915675]

Gabernet L, Jadhav SP, Feldman DE, Carandini M, Scanziani M. Somatosensory integration controlled by dynamic thalamocortical feed-forward inhibition. Neuron. 2005; 48:315–327. [PubMed: 16242411]

Galarreta M, Hestrin S. Frequency-dependent synaptic depression and the balance of excitation and inhibition in the neocortex. Nature neuroscience. 1998; 1:587–594. [PubMed: 10196566]

Glickfeld LL, Scanziani M. Distinct timing in the activity of cannabinoid-sensitive and cannabinoid-insensitive basket cells. Nature neuroscience. 2006; 9:807–815. [PubMed: 16648849]

Gogolla N, Leblanc JJ, Quast KB, Sudhof TC, Fagiolini M, Hensch TK. Common circuit defect of excitatory-inhibitory balance in mouse models of autism. J Neurodev Disord. 2009; 1:172–181. [PubMed: 20664807]

Grantyn R, Henneberger C, Juttner R, Meier JC, Kirischuk S. Functional hallmarks of GABAergic synapse maturation and the diverse roles of neurotrophins. Front Cell Neurosci. 2011; 5:13. [PubMed: 21772813]

Hussain RJ, Carpenter DO. Development of synaptic responses and plasticity at the SC-CA1 and MF-CA3 synapses in rat hippocampus. Cell Mol Neurobiol. 2001; 21:357–368. [PubMed: 11775066]

Ingram RA, Fitzgerald M, Baccei ML. Developmental changes in the fidelity and short-term plasticity of GABAergic synapses in the neonatal rat dorsal horn. J Neurophysiol. 2008; 99:3144–3150. [PubMed: 18400957]

Isaacson JS, Scanziani M. How inhibition shapes cortical activity. Neuron. 2011; 72:231–243. [PubMed: 22017986]

Isokawa M, Alger BE. Retrograde endocannabinoid regulation of GABAergic inhibition in the rat dentate gyrus granule cell. The Journal of physiology. 2005; 567:1001–1010. [PubMed: 16037085]

Jiang L, Sun S, Nedergaard M, Kang J. Paired-pulse modulation at individual GABAergic synapses in rat hippocampus. The Journal of physiology. 2000; 523(Pt 2):425–439. [PubMed: 10699086]

Kajiwara R, Wouterlood FG, Sah A, Boekel AJ, Baks-te Bulte LT, Witter MP. Convergence of entorhinal and CA3 inputs onto pyramidal neurons and interneurons in hippocampal area CA1--an anatomical study in the rat. Hippocampus. 2008; 18:266–280. [PubMed: 18000818]

Karnup S, Stelzer A. Temporal overlap of excitatory and inhibitory afferent input in guinea-pig CA1 pyramidal cells. The Journal of physiology. 1999; 516(Pt 2):485–504. [PubMed: 10087347]

Katona G, Kaszas A, Turi GF, Hajos N, Tamas G, Vizi ES, Rozsa B. Roller Coaster Scanning reveals spontaneous triggering of dendritic spikes in CA1 interneurons. Proceedings of the National Academy of Sciences of the United States of America. 2011; 108:2148–2153. [PubMed: 21224413]

Kehrer C, Maziashvili N, Dugladze T, Gloveli T. Altered Excitatory-Inhibitory Balance in the NMDA-Hypofunction Model of Schizophrenia. Front Mol Neurosci. 2008; 1:6. [PubMed: 18946539]

Kispersky TJ, Fernandez FR, Economo MN, White JA. Spike resonance properties in hippocampal O-LM cells are dependent on refractory dynamics. The Journal of neuroscience : the official journal of the Society for Neuroscience. 2012; 32:3637–3651. [PubMed: 22423087]

Klausberger T. GABAergic interneurons targeting dendrites of pyramidal cells in the CA1 area of the hippocampus. The European journal of neuroscience. 2009; 30:947–957. [PubMed: 19735288]

Klausberger T, Somogyi P. Neuronal diversity and temporal dynamics: the unity of hippocampal circuit operations. Science. 2008; 321:53–57. [PubMed: 18599766]

Klyachko VA, Stevens CF. Excitatory and feed-forward inhibitory hippocampal synapses work synergistically as an adaptive filter of natural spike trains. PLoS Biol. 2006; 4:e207. [PubMed: 16774451]

Kreitzer AC, Regehr WG. Cerebellar depolarization-induced suppression of inhibition is mediated by endogenous cannabinoids. J Neurosci. 2001; 21:RC174. [PubMed: 11588204]

Lamsa K, Heeroma JH, Kullmann DM. Hebbian LTP in feed-forward inhibitory interneurons and the temporal fidelity of input discrimination. Nature neuroscience. 2005; 8:916–924. [PubMed: 15937481]

Leung LS, Fu XW. Factors affecting paired-pulse facilitation in hippocampal CA1 neurons in vitro. Brain research. 1994; 650:75–84. [PubMed: 7953680]

Liu YC, Cheng JK, Lien CC. Rapid dynamic changes of dendritic inhibition in the dentate gyrus by presynaptic activity patterns. The Journal of neuroscience : the official journal of the Society for Neuroscience. 2014; 34:1344–1357. [PubMed: 24453325]

Luna VM, Schoppa NE. GABAergic circuits control input-spike coupling in the piriform cortex. The Journal of neuroscience : the official journal of the Society for Neuroscience. 2008; 28:8851–8859. [PubMed: 18753387]

Maccaferri G, Dingledine R. Control of feedforward dendritic inhibition by NMDA receptor-dependent spike timing in hippocampal interneurons. J Neurosci. 2002; 22:5462–5472. [PubMed: 12097498]

Maccaferri G, Roberts JD, Szucs P, Cottingham CA, Somogyi P. Cell surface domain specific postsynaptic currents evoked by identified GABAergic neurones in rat hippocampus in vitro. The Journal of physiology. 2000; 524(Pt 1):91–116. [PubMed: 10747186]

Marder CP, Buonomano DV. Differential effects of short- and long-term potentiation on cell firing in the CA1 region of the hippocampus. The Journal of neuroscience : the official journal of the Society for Neuroscience. 2003; 23:112–121. [PubMed: 12514207]

McQuiston AR. Layer selective presynaptic modulation of excitatory inputs to hippocampal cornu Ammon 1 by mu-opioid receptor activation. Neuroscience. 2008; 151:209–221. [PubMed: 18065149]

Miles R. Synaptic excitation of inhibitory cells by single CA3 hippocampal pyramidal cells of the guinea-pig in vitro. J Physiol (Lond). 1990; 428:61–77. [PubMed: 2231426]

Ohliger-Frerking P, Wiebe SP, Staubli U, Frerking M. GABA(B) receptor-mediated presynaptic inhibition has history-dependent effects on synaptic transmission during physiologically relevant spike trains. J Neurosci. 2003; 23:4809–4814. [PubMed: 12832501]

Otmakhov N, Shirke AM, Malinow R. Measuring the impact of probabilistic transmission on neuronal output. Neuron. 1993; 10:1101–1111. [PubMed: 8318231]

Owen SF, Tuncdemir SN, Bader PL, Tirko NN, Fishell G, Tsien RW. Oxytocin enhances hippocampal spike transmission by modulating fast-spiking interneurons. Nature. 2013; 500:458–462. [PubMed: 23913275]

Pitler TA, Alger BE. Depolarization-induced suppression of GABAergic inhibition in rat hippocampal pyramidal cells: G protein involvement in a presynaptic mechanism. Neuron. 1994; 13:1447–1455. [PubMed: 7993636]

Pouille F, Marin-Burgin A, Adesnik H, Atallah BV, Scanziani M. Input normalization by global feedforward inhibition expands cortical dynamic range. Nature neuroscience. 2009; 12:1577–1585. [PubMed: 19881502]

Pouille F, Scanziani M. Enforcement of temporal fidelity in pyramidal cells by somatic feed-forward inhibition. Science. 2001; 293:1159–1163. [PubMed: 11498596]

Pouille F, Scanziani M. Routing of spike series by dynamic circuits in the hippocampus. Nature. 2004; 429:717–723. [PubMed: 15170216]

Ramoa AS, Sur M. Short-term synaptic plasticity in the visual cortex during development. Cereb Cortex. 1996; 6:640–646. [PubMed: 8670689]

Sasaki T, Kimura R, Tsukamoto M, Matsuki N, Ikegaya Y. Integrative spike dynamics of rat CA1 neurons: a multineuronal imaging study. The Journal of physiology. 2006; 574:195–208. [PubMed: 16613875]

Speed HE, Dobrunz LE. Developmental decrease in short-term facilitation at Schaffer collateral synapses in hippocampus is mGluR1 sensitive. Journal of neurophysiology. 2008; 99:799–813. [PubMed: 18032567]

Speed HE, Dobrunz LE. Developmental changes in short-term facilitation are opposite at temporoammonic synapses compared to Schaffer collateral synapses onto CA1 pyramidal cells. Hippocampus. 2009; 19:187–204. [PubMed: 18777561]

Sun HY, Bartley AF, Dobrunz LE. Calcium-permeable presynaptic kainate receptors involved in excitatory short-term facilitation onto somatostatin interneurons during natural stimulus patterns. Journal of neurophysiology. 2009; 101:1043–1055. [PubMed: 19073817]

Sun HY, Dobrunz LE. Presynaptic kainate receptor activation is a novel mechanism for target cell-specific short-term facilitation at Schaffer collateral synapses. The Journal of neuroscience : the official journal of the Society for Neuroscience. 2006; 26:10796–10807. [PubMed: 17050718]

Sun HY, Lyons SA, Dobrunz LE. Mechanisms of target-cell specific short-term plasticity at Schaffer collateral synapses onto interneurones versus pyramidal cells in juvenile rats. The Journal of physiology. 2005; 568:815–840. [PubMed: 16109728]

Takacs VT, Klausberger T, Somogyi P, Freund TF, Gulyas AI. Extrinsic and local glutamatergic inputs of the rat hippocampal CA1 area differentially innervate pyramidal cells and interneurons. Hippocampus. 2012; 22:1379–1391. [PubMed: 21956752]

Thompson SM, Gahwiler BH. Activity-dependent disinhibition. I. Repetitive stimulation reduces IPSP driving force and conductance in the hippocampus in vitro. Journal of neurophysiology. 1989; 61:501–511. [PubMed: 2709096]

Torborg CL, Nakashiba T, Tonegawa S, McBain CJ. Control of CA3 output by feedforward inhibition despite developmental changes in the excitation-inhibition balance. The Journal of neuroscience : the official journal of the Society for Neuroscience. 2010; 30:15628–15637. [PubMed: 21084618]

Tsukada M, Aihara T, Kobayashi Y, Shimazaki H. Spatial analysis of spike-timing-dependent LTP and LTD in the CA1 area of hippocampal slices using optical imaging. Hippocampus. 2005; 15:104–109. [PubMed: 15390160]

Varela JA, Song S, Turrigiano GG, Nelson SB. Differential depression at excitatory and inhibitory synapses in visual cortex. The Journal of neuroscience : the official journal of the Society for Neuroscience. 1999; 19:4293–4304. [PubMed: 10341233]

Venkataraman Y, Bartlett EL. Postnatal development of synaptic properties of the GABAergic projection from the inferior colliculus to the auditory thalamus. J Neurophysiol. 2013; 109:2866–2882. [PubMed: 23536710]

Wehr M, Zador AM. Balanced inhibition underlies tuning and sharpens spike timing in auditory cortex. Nature. 2003; 426:442–446. [PubMed: 14647382]

Wierenga CJ, Wadman WJ. Excitatory inputs to CA1 interneurons show selective synaptic dynamics. Journal of neurophysiology. 2003; 90:811–821. [PubMed: 12904494]

Williams SR, Mitchell SJ. Direct measurement of somatic voltage clamp errors in central neurons. Nature neuroscience. 2008; 11:790–798. [PubMed: 18552844]

Wilson RI, Nicoll RA. Endogenous cannabinoids mediate retrograde signalling at hippocampal synapses. Nature. 2001; 410:588–592. [PubMed: 11279497]

Zachariou M, Alexander SP, Coombes S, Christodoulou C. A biophysical model of endocannabinoid-mediated short term depression in hippocampal inhibition. PloS one. 2013; 8:e58926. [PubMed: 23527052]

Zemankovics R, Veres JM, Oren I, Hajos N. Feedforward inhibition underlies the propagation of cholinergically induced gamma oscillations from hippocampal CA3 to CA1. The Journal of neuroscience : the official journal of the Society for Neuroscience. 2013; 33:12337–12351. [PubMed: 23884940]

Zhang L, Spigelman I, Carlen PL. Development of GABA-mediated, chloride-dependent inhibition in CA1 pyramidal neurones of immature rat hippocampal slices. The Journal of physiology. 1991; 444:25–49. [PubMed: 1822551]

Zhang Z, Jiao YY, Sun QQ. Developmental maturation of excitation and inhibition balance in principal neurons across four layers of somatosensory cortex. Neuroscience. 2011; 174:10–25. [PubMed: 21115101]

Zucker RS, Regehr WG. Short-term synaptic plasticity. Annu Rev Physiol. 2002; 64:355–405. [PubMed: 11826273]

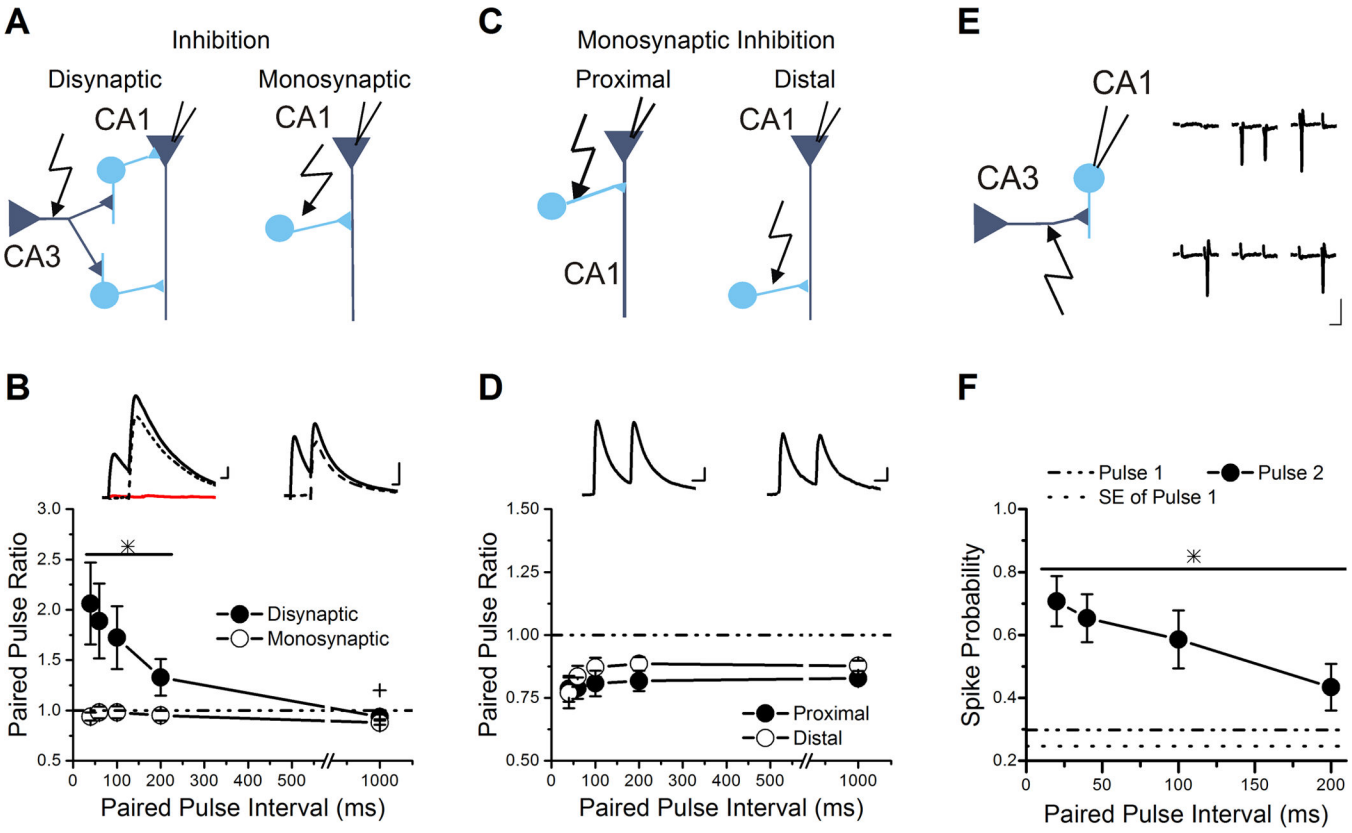

Figure 1. Disynaptic inhibition shows paired-pulse facilitation due to recruitment of interneurons

A, Schematics for recordings of disynaptic inhibition (left) and monosynaptic inhibition (right), with interneurons as circles and pyramidal neurons as triangles.

B, Group results for paired-pulse ratios of IPSCs plotted against the paired-pulse interval show that disynaptic inhibition facilitates (n=18) while monosynaptic inhibition depresses (n=16). The line and * over a subset of data points indicates the values that are significantly different from monosynaptic inhibition and from baseline. The + over the 1000 ms interval of disynaptic inhibition indicates that the value is significantly different from baseline and expresses slight paired-pulse depression. Inset: Example traces of disynaptic (left) and monosynaptic (right) IPSCs recorded from pyramidal neurons held at 0 mV to remove the AMPA receptor component and isolate the inhibitory current. Disynaptic inhibition is blocked by application of 10 μM NBQX (flat line on the left insert). Solid lines are original traces and dashed lines are the traces after subtraction of the first pulse. Scale Bars: 20 ms, 50 pA (top), 50 pA (bottom).

C, Schematic for recordings of monosynaptic inhibiton from proximal and distal stimulation.

D, Group results for paired-pulse ratios of monosynaptic IPSCs plotted against the paired-pulse interval for proximal (open triangle, n=11) and distal (closed diamond, n=8) stimulation. No significant difference was seen. Inset: Example traces of proximal (left) and distal (right) monosynaptic IPSCs. Scale Bars: 20 ms, 25 pA

E, Left: Schematic of the cell-attached recording of *s. radiatum* interneurons. Right: Example traces from cell-attached recording onto an interneuron in *s. radiatum* during paired-pulse stimulation at 100 ms interval show responses with spikes and no spike. Stimulus artifacts have been removed. Traces are in chronological order, but are not sequential, because trials cycled through a series of paired-pulse intervals, so there were intervening trials at different intervals (not shown). Scale Bars: 20 ms, 5 pA.
F, Group results for the spike probability plotted against the paired-pulse interval (n=11). The spike probability is enhanced 2-fold at the shorter paired-pulse intervals compared to the spike probability on the first pulse. The line and * over the data points indicates the values that are significantly different from pulse 1.

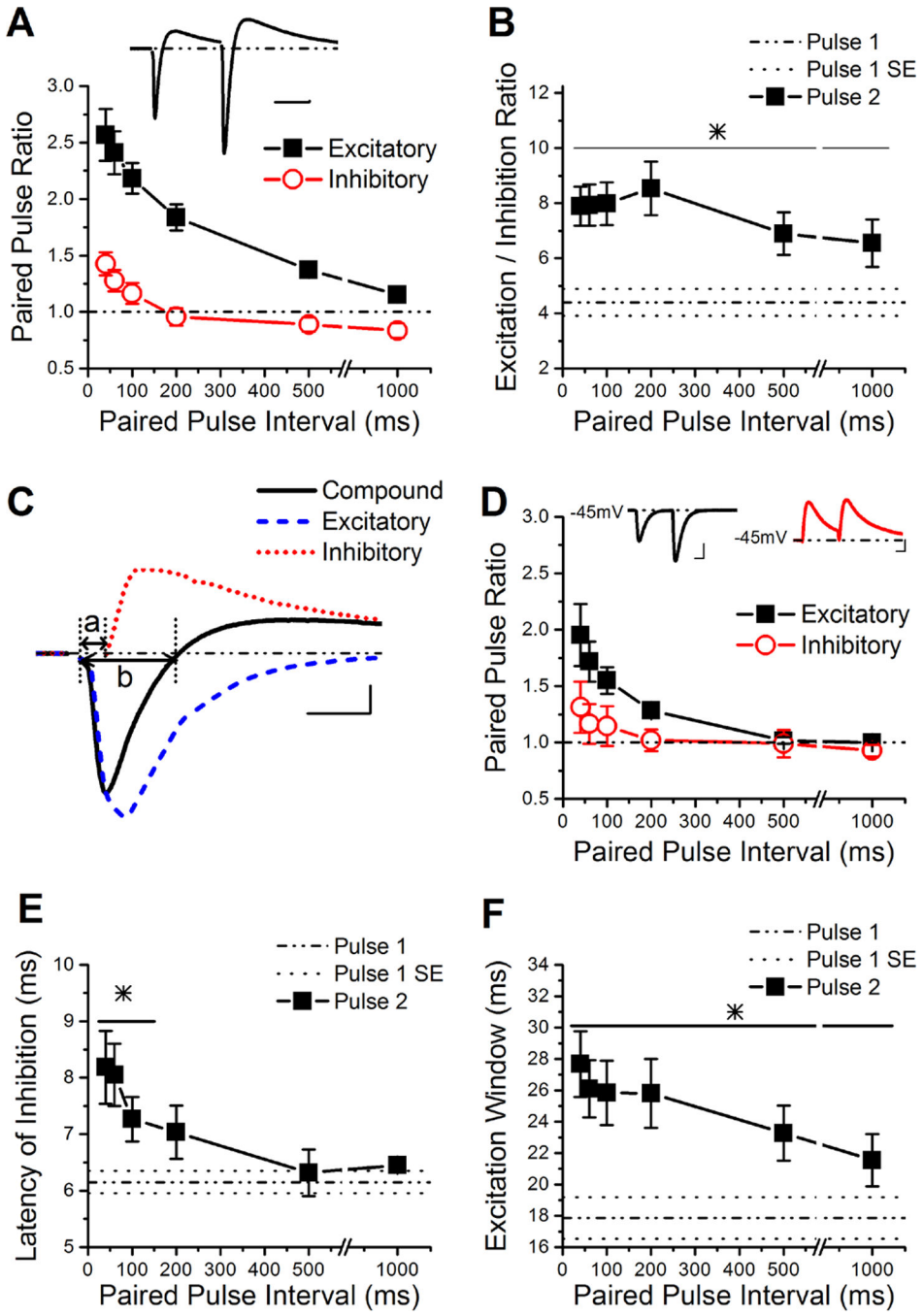

Figure 2. The E/I ratio is dynamically enhanced by short-term plasticity

A, Group results for the paired-pulse ratios of the peaks of the excitatory and inhibitory components of the compound PSC (n=14). Inset: Example trace of the compound PSC in a CA1 pyramidal cell held at −45 mV. Scale Bars: 50 ms, 50 pA.

B, Group results for the E/I ratio determined from the peak of the compound PSC (n=14). The line and * over the data points indicates the values that are significantly different from pulse 1.

C, Example trace of a single compound PSC (solid line), the underlying excitatory response (in bicuculline, dashed line), and the underlying inhibitory response (obtained through subtraction of the underlying excitatory response from the compound PSC, dotted line). The latency of inhibition is measured as the time from the stimulus artifact until the onset of inhibition, as is depicted by line a. The excitation window was determined by the width of the excitatory component of the compound at the points that it crosses 0 pA, as depicted by line b (Chittajallu *et al.*, 2012). Scale Bars: 10 ms, 125 pA.

D, Group results for the paired-pulse ratio of the underlying excitatory and inhibitory responses, based on peak values (n=6). Insets: Left, example trace of the underlying EPSC response obtained from the wash in of the $GABA_AR$ antagonist bicuculline. Right, example trace of the underlying IPSC response obtained from subtraction of the bicuculline trace from the compound trace. Scale Bars: 25ms, 250 pA (left), 150 pA (right).

E, The delay for inhibition is calculated from the subtracted underlying inhibitory traces, the region is depicted in **C** by line a. The group results show that inhibition is delayed dependent on the paired-pulse interval (n=6). The line and * over the data points indicates the values that are significantly different from pulse 1.

F, Group results for the time window for excitation available during the compound PSC (n=14), measured as shown in **C**. The line and * over the data points indicates the values that are significantly different from pulse 1.

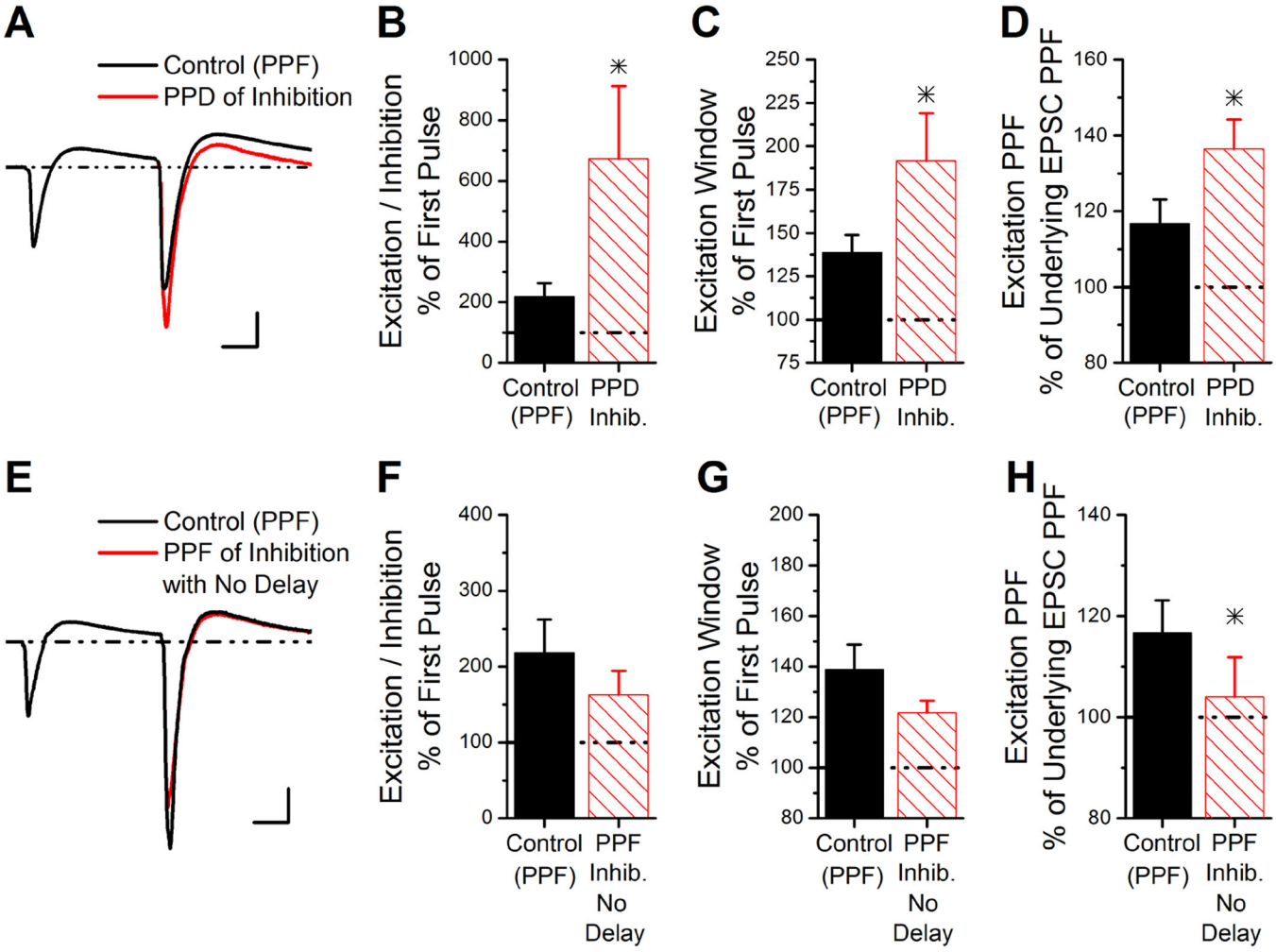

Figure 3. Simulated compound PSCs predict greatly enhanced E/I ratio if inhibition had paired-pulse depression instead of facilitation

A, The simulated compound trace is generated from the average of individual experiments based on the summation of the underlying EPSC and IPSC traces at a paired-pulse interval of 100 ms. The simulated compound trace is shown from summation of the underlying EPSC with either a facilitating IPSC (control) or depressing IPSC (PPD of inhibition). The paired-paired pulse ratio of the underlying IPSC was 0.77 for the simulated PSC with paired-pulse depression of inhibition, similar to the average paired-pulse ratios of monosynaptic inhibition measured at −45 mV. Scale Bars: 10 ms, 125 pA.

B, The E/I ratio on the second pulse of the simulated compound PSCs (as in Figure 4A) with PPF of inhibition or PPD of inhibition, shown as a percent of the E/I ratio from the first pulse (n=6).

C, The duration of the excitation window on the second pulse of the simulated compound PSCs with PPF of inhibition or PPD of inhibition, shown as a percent of the excitation window on the first pulse (n=6).

D, The PPF of the excitatory component of the simulated compound PSCs with PPF of inhibition or PPD of inhibition, shown as a percent of the paired-pulse ratio of the underlying EPSC.

E, The simulated compound trace is generated from the average of individual experiments based on the summation of the underlying EPSC and IPSC traces at a paired-pulse interval of 100 ms. The timing of the underlying IPSC on the second pulse was shifted to match the onset of the first pulse, thereby generating compound PSCs with no delay in inhibition, but maintaining the facilitation of inhibition (PPF of inhibition with no delay). Scale Bars: 10 ms, 125 pA.

F, The E/I ratio on the second pulse of the simulated compound PSCs from Figure 4E without or with a delay in the onset of inhibition, shown as a percent of the E/I ratio from the first pulse.

G, The duration of the excitation window on the second pulse of the simulated compound PSCs without or with a delay in the onset of inhibition, shown as a percent of the excitation window on the first pulse.

H, The PPF of excitation of the simulated compound PSCs without or with a delay in the onset of inhibition, shown as a percent of the paired-pulse ratio of the underlying EPSC.

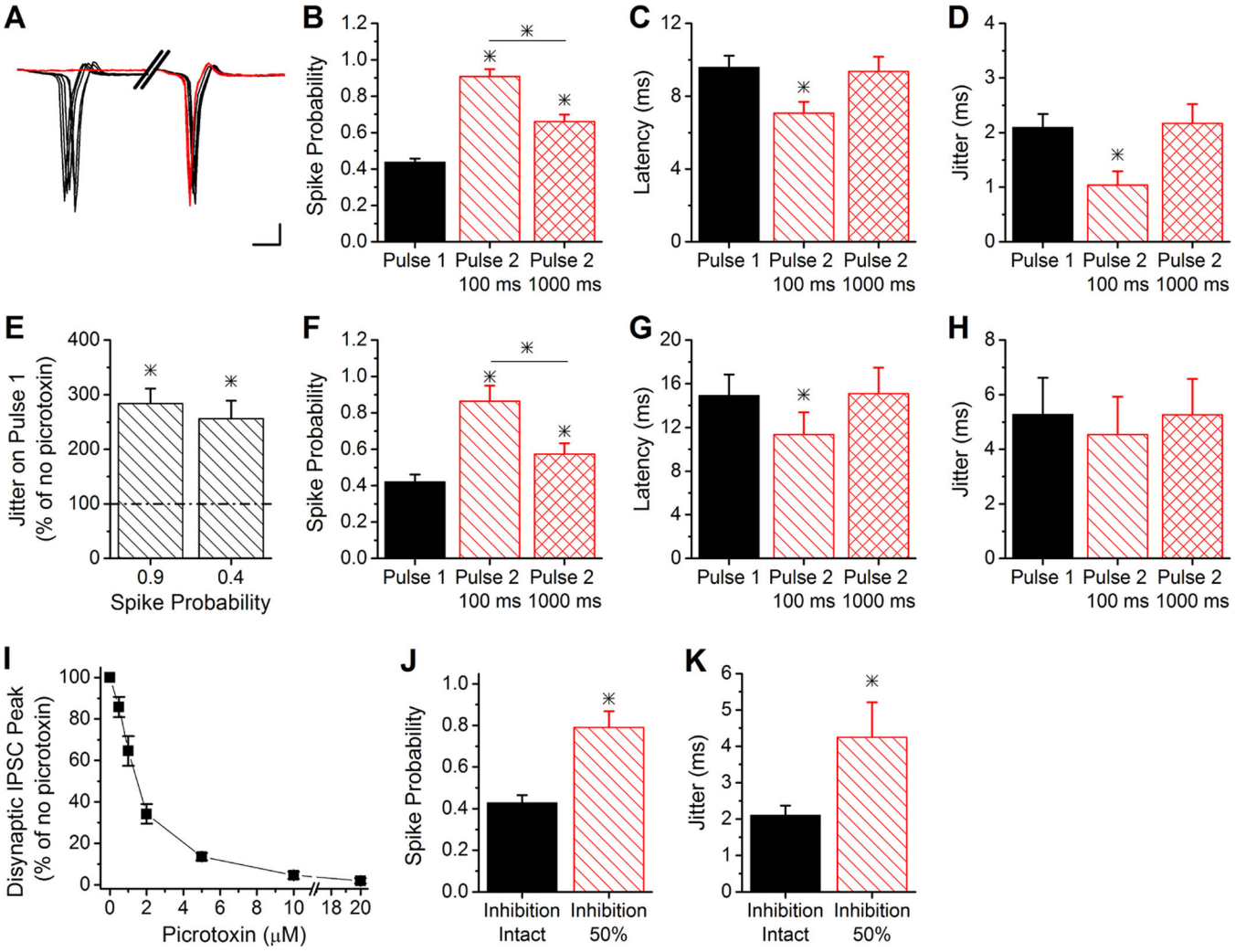

Figure 4. Short-term plasticity modulates spiking of CA1 pyramidal cells

A, Example traces from cell-attached recordings demonstrating that paired-pulse stimulation decreased the jitter of CA1 pyramidal cell spiking at the 100 ms interval. Note the break in the x axis. Scale bars: 2 ms, 50 pA.

B, Group results for the spike probability of pulse 1 and pulse 2 at 100 ms and 1000 ms paired-pulse intervals (n=11). * indicates difference from pulse 1. The line and * indicates difference between the second pulse intervals.

C, Group results for the spike latency of pulse 1 and pulse 2 at 100 ms and 1000 ms paired-pulse intervals (n=11). * indicates difference from pulse 1 and pulse 2 at 1000 ms.

D, Group results for the spike jitter of pulse 1 and pulse 2 at 100 ms and 1000 ms paired-pulse intervals (n=11). * indicates difference from pulse 1 and pulse 2 at 1000 ms.

E, Group results of spike jitter on pulse 1 of experiments in 100 μM picrotoxin, at same stimulus intensity as with no picrotoxin (spike probability = 0.85) and with stimulation strength reduced (spike probability 0.4), as a percentage of jitter with no picrotoxin (n=4). * indicates difference from no picrotoxin.

F–H, Same as **B–D**, except with 100 μM picrotoxin and stimulation strength reduced to produce same spike probability on pulse 1 as without picrotoxin **(B)** (n=4).

I, Dose response curve for disynaptic IPSC amplitude at different concentrations of picrotoxin (n=4).

J, Spike probability on pulse 1 with 1.5 μM picrotoxin (inhibition 50%) and no picrotoxin (inhibition intact) at same stimulus intensity (n=5). * indicates difference from inhibition intact.

K, Spike jitter on pulse 1 with 1.5 μM picrotoxin (inhibition 50%) and no picrotoxin (inhibition intact) at same stimulus intensity (n=5). * indicates difference from inhibition intact.

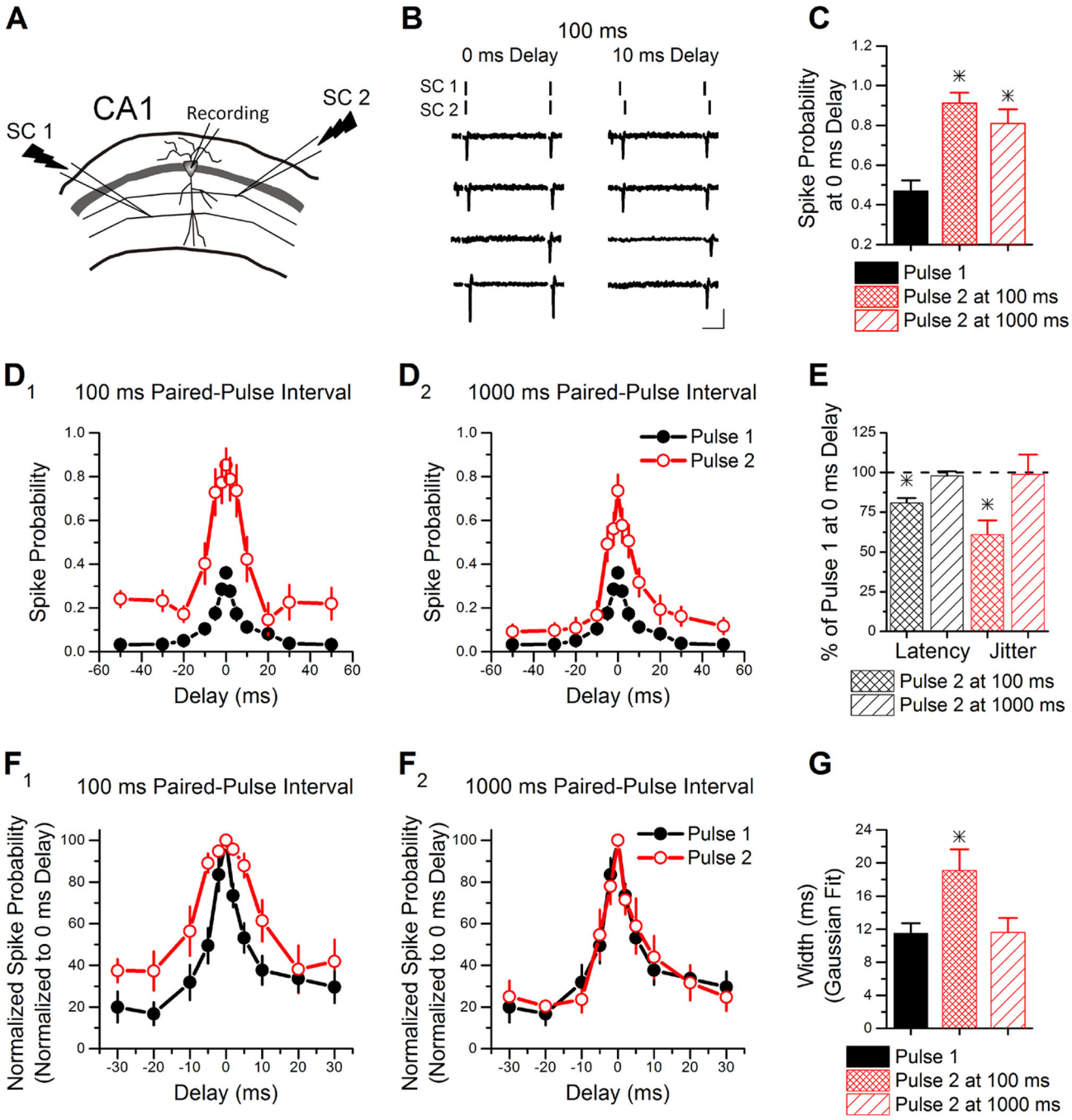

Figure 5. Modulation of the spike integration window by short-term plasticity

A, Schematic of the two independent Schaffer collateral stimulation pathways used to determine the spike integration of a CA1 pyramidal cell.

B, Example traces from cell-attached recordings at a paired-pulse interval of 100 ms. The lines at the top of each column indicate the stimulation timing in each Schaffer collateral pathway. On the left are traces in which both pathways are simultaneously stimulated (0 ms delay). On the right are traces in which the delay between the two Schaffer collateral pathways is 10 ms. Scale bars: 25 ms, 15 pA.

C, Group results for the spike probability of pulse 1 and pulse 2 at 100 ms and 1000 ms when both pathways are simultaneously stimulated. * indicates difference from pulse 1
D, Group results for the spike probability plotted against the delay of the second stimulus show that short-term plasticity enhances the spike probability of second pulse compared to the first pulse. D_1 compares the first pulse (n=14) and the second pulse at 100 ms (n=8). D_2 compares the first pulse and the second pulse at 1000 ms (n=6).
E, Group results for spike latency and jitter on pulse 2 as a percentage of pulse 1 for stimulation of the two pathways with 0 ms delay. * indicates difference from pulse 1.
F, Group results for the normalized spike probability plotted against the delay for the 100 ms interval (F_1) and the 1000 ms interval (F_2).
G, Group results for the Gaussian fit width of pulse 1 and pulse 2 at 100 ms and 1000 ms. This indicates that the integration window is broader on the second pulse at the 100 ms interval but not the 1000 ms interval. * indicates difference from pulse 1 and pulse 2 at 1000 ms interval.

Table 1

Properties of Schaffer collateral evoked disynaptic IPSCs vs monosynaptic IPSCs on pulse 1

	Disynaptic IPSC (n=18)	Monosynaptic IPSC (n=16)
IPSC Amplitude (pA)	103.9 ± 24.6	53.1 ± 14.2
Charge	5325 ± 1283	2788 ± 713
Latency (ms)	***8.12 ± 0.91***	***5.38 ± 0.44****
Time to Peak (ms)	12.11 ± 0.98	11.46 ± 0.53
20% to 80% Rise Time (ms)	4.96 ± 0.47	4.42 ± 0.27
Tau Decay (ms)	36.29 ± 3.40	39.19 ± 2.99
Half-Width (ms)	39.36 ± 3.23	40.42 ± 2.53

Table 2

Properties of Schaffer collateral evoked disynaptic IPSCs in response to short-term plasticity

	DS Pulse 2 at 40ms	DS Pulse 2 at 60ms	DS Pulse 2 at 100ms	DS Pulse 2 at 200ms	DS Pulse 2 at 1000ms
Latency (ms)	***9.15 ± 0.91****	***8.77 ± 0.89****	***8.60 ± 0.87****	*8.43 ± 0.87*	*8.07 ± 0.86*
Time to Peak (ms)	13.32 ± 1.62	12.88 ± 1.35	12.58 ± 1.21	12.48 ± 1.14	12.63 ± 1.18
20% to 80% Rise Time (ms)	5.08 ± 0.59	4.91 ± 0.55	4.82 ± 0.56	4.98 ± 0.55	4.98 ± 0.53
Tau Decay (ms)	50.91 ± 12.45	47.36 ± 9.96	43.3 ± 7.05	39.54 ± 4.58	37.35 ± 2.92
Half-Width (ms)	49.41 ± 7.38	46.46 ± 6.51	42.42 ± 5.30	39.95 ± 4.12	37.83 ± 3.13

The data were obtained from a total of 18 pyramidal cells. DS stands for disynaptic IPSCs.

Asterisk indicates significantly different from first pulse.